



HAL
open science

Structure-rheology properties of polyethylenes with varying macromolecular architectures

Jixiang Li, Ibtissam Touil, Carlos Fernandez-De-Alba, Fernande Boisson-da Cruz, Olivier Boyron, Esmaeil Narimissa, Bo Lu, Huagui Zhang, Abderrahim Maazouz, Khalid Dr. Lamnawar

► **To cite this version:**

Jixiang Li, Ibtissam Touil, Carlos Fernandez-De-Alba, Fernande Boisson-da Cruz, Olivier Boyron, et al.. Structure-rheology properties of polyethylenes with varying macromolecular architectures. *Journal of Polymer Research*, 2023, 30 (12), pp.454. 10.1007/s10965-023-03838-9 . hal-04477516

HAL Id: hal-04477516

<https://hal.science/hal-04477516v1>

Submitted on 26 Feb 2024

HAL is a multi-disciplinary open access archive for the deposit and dissemination of scientific research documents, whether they are published or not. The documents may come from teaching and research institutions in France or abroad, or from public or private research centers.

L'archive ouverte pluridisciplinaire **HAL**, est destinée au dépôt et à la diffusion de documents scientifiques de niveau recherche, publiés ou non, émanant des établissements d'enseignement et de recherche français ou étrangers, des laboratoires publics ou privés.

Journal of Polymer Research

Structure-rheology Properties of Polyethylenes with Varying Macromolecular Architectures

--Manuscript Draft--

| | | |
|--|--|---------------------|
| Manuscript Number: | JPOL-D-23-01129 | |
| Full Title: | Structure-rheology Properties of Polyethylenes with Varying Macromolecular Architectures | |
| Article Type: | Manuscript | |
| Keywords: | low-density polyethylene, long-chain branching, relationships between molecular structures and rheological properties | |
| Corresponding Author: | Khalid Lamnawar INSA Lyon: Institut National des Sciences Appliquees de Lyon FRANCE | |
| Order of Authors: | Jixiang Li Ibtissam Touil Carlos Fernández de Alba Fernande Boisson Olivier Boyron Esmaeil Narimissa Bo Lu Huagui Zhang Abderrahim Maazouz Khalid Lamnawar | |
| Corresponding Author Secondary Information: | | |
| Corresponding Author's Institution: | INSA Lyon: Institut National des Sciences Appliquees de Lyon | |
| Corresponding Author's Secondary Institution: | | |
| First Author: | Jixiang Li | |
| First Author Secondary Information: | | |
| Order of Authors Secondary Information: | | |
| Funding Information: | Agence Nationale de la Recherche (ANR-20-CE06-0003) | Pro Khalid Lamnawar |
| Abstract: | It is proverbial that the rheological properties of low-density polyethylene (LDPE) and linear low-density polyethylene (LLDPE) are disparate because of their different molecular microstructures due to the unlike methods of polymerization. In this work, multiple characterizations including Size-Exclusion Chromatography (SEC) coupled with low-angle light scattering and viscosimeter, ¹³ C Nuclear Magnetic Resonance, Crystallization Elution Fractionation (CEF) and Differential Scanning Calorimetry (DSC) were conducted to get detailed information of branching on different LDPEs and LLDPEs. It was found that, in our case, LDPEs possessed higher molecular weight and greater amounts of long-chain branching (LCB) in comparison with LLDPEs. The Chemical Composition Distribution (CCD) of each LLDPE sample depends strongly on the catalyst used. LLDPE produced by Z-N catalyst exhibited broad short-chain branching (SCB) distribution (less uniform composition distribution), whereas LLDPE obtained by metallocene catalyst showed more uniform microstructure. Unlikely, the two LDPEs displayed wider but unimodal distribution corresponding to the free-radical polymerization mechanism. Both linear and nonlinear rheological results were strongly | |

| | |
|------------------------------------|--|
| | <p>influenced by the presence of LCB. LDPEs in this work exhibited higher zero shear-viscosity, higher values of storage modulus, longer relaxation times, and higher activation energy comparing to LLDPEs. The presence of LCB leads to more pronounced strain hardening behavior in the elongational flow which is neglected in LLDPE. The molecular structures of linear and branched PEs were consistent with the rheological properties.</p> |
| <p>Suggested Reviewers:</p> | <p>Abdellah Ajji Polytechnique Montreal abdellah.ajji@polymtl.ca</p> |
| | <p>Ehsan Behzadfar Toronto Metropolitan University behzadfar@torontomu.ca</p> |
| | <p>Peter Halley UQ: The University of Queensland p.halley@uq.edu.au</p> |
| | <p>Quan Chen Changchun Institute of Applied Chemistry Chinese Academy of Sciences: Chang Chun Institute of Applied Chemistry Chinese Academy of Sciences qchen@ciac.ac.cn</p> |

[Click here to view linked References](#)

Structure-rheology Properties of Polyethylenes with Varying Macromolecular Architectures

Jixiang Li^a, Ibtissam Touil^a, Carlos Fernández de Alba^a, Fernande Boisson^a, Olivier Boyron^b, Esmail Narimissa^c, Bo Lu^d, Huagui Zhang^e, Abderrahim Maazouz^{a,f}, Khalid Lamnawar^{a,*}

^a *Université de Lyon, CNRS, UMR 5223, Ingénierie des Matériaux Polymères, INSA Lyon, F-69621, Villeurbanne, France*

^b *Université de Lyon, CNRS, UMR 5223, Ingénierie des Matériaux Polymères, UCBL, F-69621, Villeurbanne, France*

^c *Dept. of Chemical Engineering, Guangdong Technion–Israel Institute of Technology (GTIIT), Shantou 515063, China*

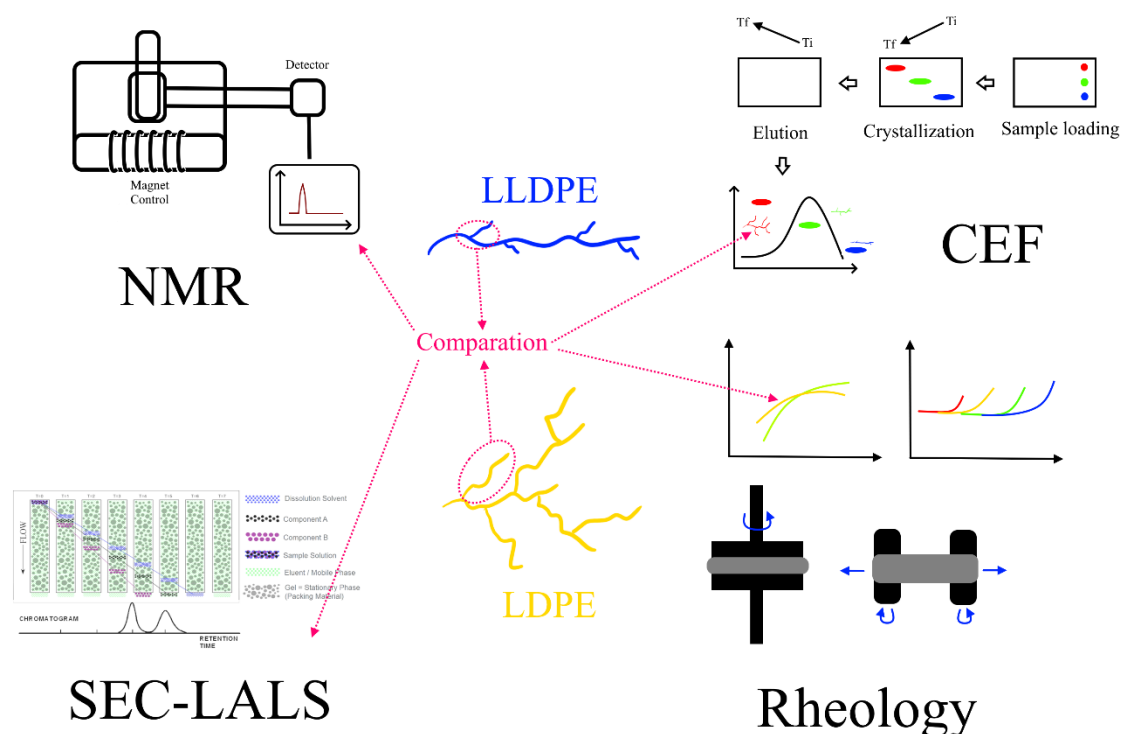
^d *Key Laboratory of Materials Processing and Mold (Ministry of Education), National Engineering Research Center for Advanced Polymer Processing Technology, Zhengzhou University, Zhengzhou 450002, China*

^e *College of Chemistry and Materials Science, Fujian Key Laboratory of Polymer Materials, Fujian Provincial Key Laboratory of Advanced Materials Oriented Chemical Engineering, Fujian Normal University, Fuzhou 350007, China*

^f *Hassan II Academy of Science and Technology, 10100 Rabat, Morocco*

* *Corresponding author. E-mail address: khalid.lamnawar@insa-lyon.fr (K. Lamnawar).*

Graphical abstract



Abstract

It is proverbial that the rheological properties of low-density polyethylene (LDPE) and linear low-density polyethylene (LLDPE) are disparate because of their different molecular microstructures due to the unlike methods of polymerization. In this work, multiple characterizations including Size-Exclusion Chromatography (SEC) coupled with low-angle light scattering and viscosimeter, ^{13}C Nuclear Magnetic Resonance, Crystallization Elution Fractionation (CEF) and Differential Scanning Calorimetry (DSC) were conducted to get detailed information of branching on different LDPEs and LLDPEs. It was found that, in our case, LDPEs possessed higher molecular weight and greater amounts of long-chain branching (LCB) in comparison with LLDPEs. The Chemical Composition Distribution (CCD) of each LLDPE sample depends strongly on the catalyst used. LLDPE produced by Z-N catalyst exhibited broad short-chain branching (SCB) distribution (less uniform composition distribution), whereas LLDPE obtained by metallocene catalyst showed more uniform microstructure. Unlikely, the two LDPEs displayed wider but unimodal distribution corresponding to the free-radical polymerization mechanism. Both linear and nonlinear rheological results were strongly influenced by the presence of LCB. LDPEs in this work exhibited higher zero shear-viscosity, higher values of storage modulus, longer relaxation times, and higher activation energy comparing to LLDPEs. The presence of LCB leads to more pronounced strain hardening behavior in the elongational flow which is neglected in LLDPE. The molecular structures of linear and branched PEs were consistent with the rheological properties.

Key words: low-density polyethylene, long-chain branching, relationships between molecular structures and rheological properties

1. Introduction

Polyethylene (PE), although with the simplest chemical composition of the polymer chains, is now one of the most important polymers in the world. The referred traditional application area including packaging¹, consumer goods², pipes and fittings³, electrical insulation⁴ etc. Recently it is also proved to be suitable for some advanced functional materials especially the thermal managing products^{5,6} and membranes or fibers with high mechanical properties⁷⁻⁹. Due to the uncomplicated chemical composition, the products fabricated by PE are often chemically stable which is one of the advantages as well as one of the disadvantages that is hard to realize chemical modification. Correspondingly, the processing and foaming, usually influenced by molecular weight, chain structure and crystallization, of PE become very crucial for the final properties of the products.

It is well known that according to the chain structure, the PE can be classified into three main categories: high-density polyethylene (HDPE), linear low-density polyethylene (LLDPE), and low-density polyethylene (LDPE), as illustrated in Figure 1. HDPE has a linear structure with few or no branches, which results in a high degree of crystallinity and a low-strain hardening in the melt state¹⁰. When the molecular weight of HDPE reaching a certain amount (1×10^6), it can be defined as the Ultra-high molecular weight polyethylene (UHMWPE) which is with much better mechanical properties but significantly difficult to be processed¹¹. Linear low-density polyethylenes (LLDPE) are polymerized using ethylene and an α -olefin, which is commonly 1-butene, 1-hexene, or 1-octene^{12,13}. The incorporation of a small number of long-chain branching (LCB) structures into linear polyethylene (PE) would enhance processing characteristics and their

molecular structure, physical properties, and the applications are thus broadened. LDPE, on the other hand, is often made by a free-radical process at high temperatures and pressure¹⁴. This process results in a polymer with a very wide molecular weight distribution and a complex structure containing a wide range of branching structures. LDPE contains both short-chain branches (SCBs) and long-chain branches (LCBs) that can be as long as the main chain.

It is the chain structure that leads to the quite disparate properties among the three sorts of PEs. Meanwhile, the molecular weight distribution, degree of branching, branch length as well as nature of branching existing in polymers all affect their processing behavior and rheological properties dramatically in both shear and elongational regimes¹⁵. Therefore, to better and deeper understand the relationship between chain structure of polyethylene and melt rheological properties is always necessary for better processing, since rheological performances are sensitive to molecular structures. In most cases, short-chain branches decrease crystallinity, which resulted in the low density in the solid phase and the high flexibility¹⁴. While, long-chain branches lead the viscosity to drop significantly at higher shear rates, which facilitates the processing of this material in the molten state. An increase of LCB leads to a higher zero-shear rate viscosity, sometimes even difficult to obtain a precise data of this viscosity via rheological methods¹⁶. Moreover, LCB is known to show strain hardening during elongational flow and to alter crystallization, resulting in changed mechanical properties when compared to linear structures¹⁵⁻¹⁷.

Various characterization techniques have been used to investigate the branching degree and branch length of LDPE and LLDPE chemically such as ¹³C NMR spectroscopy, SEC^{16,18-21}. C. Gabriel et al²² compared the different methods for investigation of the short chain branching in LLDPE where their highlight is that the temperature rising elution fractionation (TREF) method is more effective but not suitable for samples with highly branched structures in contrast with DSC method. More precise information of branching can be gotten from NMR test. For

instance, Zhe Zhou et al²³ used a novel solvent to conduct the ¹³C NMR test to avoid the overlap of the ethylene–hexene–ethylene branch (EHE Br) peak with the LCB methine peak in conventional solvents used for dissolving ethylene–hexene LLDPE and obtained a more precise information of LCB inside LLDPE.

In terms of rheology, Shear-thinning and melt strength can also be applied to reflected the contribution of branching, but they are unable to precisely determine the amount of branching. Seyed Hassan Jafari et al²⁴ proved the thermorheological analysis can be an effective way to qualitatively assess the LCB content in LLDPE and LDPE, which includes methods like time–temperature superposition (TTS), Cole–Cole plot, van Gorp–Palmen curve, phase angle (δ) versus reduced frequency curve, and activation energy as a function of the δ . Olivier Boyron et al²⁵ also tried to quantitatively determined the branching content in LLDPE. The content of co-monomer in LLDPEs could be determined using a calibration formulated which can only reflect the content of SCBs. Although the methods for branching are various, the collaboration between chemical characterization and rheology is remained unclear especially in nonlinear regime.

The present work firstly is devoted to giving a very detailed characterization of the molecular structure of two LLDPE and two LDPE by NMR, SEC and CEF methods. Next, the goal is dedicated to investigating the linear and nonlinear rheology of those PEs at the molten state. These findings will contribute to better understanding the relationships between the molecular structure of linear and branched PEs and their rheological properties (both linear and non-linear viscoelastic properties).

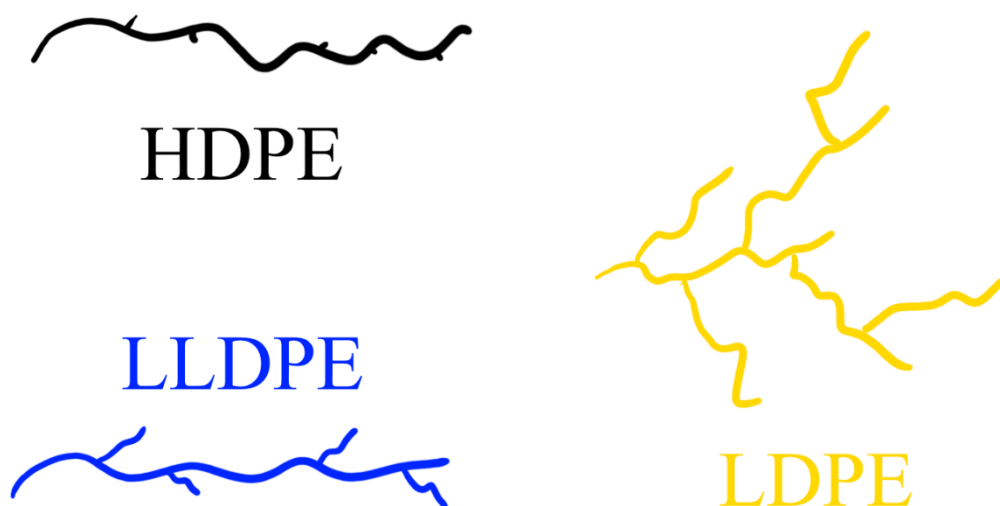


Figure 1 HDPE, LDPE, and LLDPE molecular structures.

2. Experiments

2.1 Materials

Two sets of samples were selected in view of our goals: a set of two low-density polyethylenes (LDPE) (ExxonMobil 165 and LyondellBasell 3020D) and two linear low-density polyethylenes (LLDPE) (INEOS 6910 and MarlexD139) with different molecular weights and branching architectures. The LLDPEs studied were ethylene-1-hexene copolymer produced by a Z-N catalyst (LL1) and a metallocene catalyst (LL2).

Table 1 Summary of physical characteristics of polyethylenes

| Polymer | Manufacturer | Comonomer type | Density (g/cm ³) | MFI (190°C/2.16 kg) (g/10min) |
|-------------|----------------------|----------------|------------------------------|-------------------------------|
| LDPE (L1) | ExxonMobil 165 | ----- | 0,922 | 0.3 |
| LDPE (L2) | LyonDellBasell 3020D | ----- | 0,928 | 0.3 |
| LLDPE (LL1) | Ineos 6910 | 1-Hexene | 0,936 | 1.0 |
| LLDPE (LL2) | MarlexD139 | 1-Hexene | 0,918 | 1.0 |

2.2 Characterizations

2.2.1 Shear rheology

Rheological measurements were done according to our pervious research²⁶ of the neat polymers were performed by a stress-controlled DHR-2 (Discovery Hybrid Rheometer, TA Instruments), using 25 mm parallel-plate geometry with a gap of 1 mm. The experiments were conducted at temperatures ranging from 150 to 240°C under nitrogen atmosphere. The specimens for rheological measurements were compression-molded into disks with diameter of 25mm and thickness of 1.5mm. The compression time was 5 min to reduce any residual stress with a pressure of 200 bars between two Teflon films to obtain a smooth surface. The first test was a dynamic strain sweep with a maximum angular frequency²⁷. Thus, the strain value is fixed to 5% to ensure the linear viscoelastic domain. Moreover, the following rheological tests were performed:

- 1) A dynamic time sweep test was performed to verify the thermal stability of the neat polymers at 190°C with a set angular frequency of 1 rad/s.
- 2) A dynamic frequency sweep tests with frequencies ranging from 628 to 0.01 rad/s at fixed strain amplitude of 5% from 150 to 250°C.

2.2.2 Start -up uniaxial extensional rheology

In our study, uniaxial extensional rheology measurements were carried out by a Sentamanat Extensional Rheometer fixture (SER-2, Xpansion Instruments, LLC) mounted on a DHR-2 TA instrument. The neat polymers were split into strips with dimensions of 20 mm × 10 mm × 0.8 mm (length × width × thickness). Then, the extremities of the sample were mounted on the dual rotating windup drums, to ensure a uniform extensional deformation. Therein, the extensional flow data were collected at different Hencky strain rates at constant temperatures (150°C, 190°C and 230°C) under a nitrogen atmosphere. Strain validation and continuous visual access were performed during the measurements by a built-in camera to

monitor the evolution of a specimen's width dimension at the constant Hencky strain rate. Figure shows an example of the real evolution of sample width dimension of neat polymer LL2 undergoing stretching at a constant Hencky strain rate of 0.1 s^{-1} , while Figure shows an example of theoretical width dimension. The actual sample width evolution was compared then with theoretical ones by using the eq (1):

$$W(t) = W_0[\exp(-\dot{\varepsilon}_H t)]^{1/2} \quad (1)$$

, where W_0 is the initial width dimension before stretching.

The Hencky strain rate can be expressed as:

$$\dot{\varepsilon}_H = \frac{2\Omega R}{L_0} \quad (2)$$

where R corresponds to the windup drums radius, L_0 is the fixed length of the specimen sample, and Ω represents the rotation speed of cylinders.

For a constant Hencky strain rate, the cross-sectional area of the stretched molten specimen can be expressed as:

$$A(t) = A_0 \left(\frac{\rho_s}{\rho_M}\right)^{2/3} \exp(-\dot{\varepsilon}_H t) \quad (3)$$

where ρ_M is the melt density of the polymer, ρ_s is the solid-state density and A_0 is the cross-sectional area at the solid-state. Then the tensile stress growth coefficient, $\eta_E^+(t)$ of the stretched sample can be defined as

$$\eta_E^+(t) = \frac{F(t)}{\dot{\varepsilon}_H A(t)} \quad (4)$$

2.2.3 Size-exclusion chromatography coupled with LALS and viscometer

Size exclusion chromatography is a method in which molecules are separated according to their hydrodynamic volume. The combination of Size-Exclusion Chromatography (SEC) coupled with low-angle light scattering (LALS) and

viscosimeter provides a versatile and reliable way to characterize the polymer chain microstructure (Figure S3, Supplementary Note 2).

The SEC experiments were carried out using a Viscotek system (from Malvern Instruments) equipped with three columns (PLgel Olexis 300 mm × 7 mm I.D. from Agilent Technologies). 200 μL of sample solutions with concentration of 5 mg/mL were eluted in 1,2,4-trichlorobenzene using a flow rate of 1 mL/min at 150°C. On-line detection was achieved by combining a differential refractive index detector, a low angle light scattering detector (LALS), and a viscometer. This coupling provides both absolute molecular weight measurement and structural information. OmniSEC software was used for the calculations.

The weight average molecular weight (M_w) and the number average molecular weight (M_n) were determined following the equations below:

$$\overline{M}_n = \frac{\sum n_i M_i}{\sum n_i} \quad (5)$$

$$\overline{M}_w = \frac{\sum n_i M_i M_i}{\sum n_i M_i} = \sum w_i M_i \quad (6)$$

Where w_i is the weight average molecular weight and n_i is the fraction of molecules having a molecular weight of M_i . Nuclear Magnetic Resonance ¹³C-NMR

Nuclear Magnetic Resonance is a spectrometric technique used to probe details of molecular features. The position of a peak in the ¹³C-NMR spectrum is defined by the local electronic environment of the carbon atom in the molecule²⁸. The ¹³C spectra were recorded with a Bruker Avance II spectrometer operating at 100.6 MHz for ¹³C observation, equipped with a selective ¹H/¹³C 10mm probe with z-gradient coil. Samples for NMR analysis were prepared as 5 w% solutions in a mixture of tetrachloroethylene (TCE) and deuterated benzene (TCE/C6D6 7:3 vol). Spectra were recorded at 90°C. Chemical shifts values (δ), were referenced to the signal of CH₂ methylene carbons set at $\delta=30.06$ ppm. Spectra were taken

with power gated proton decoupling sequence, a 70° rf pulse and a recycle delay time of 4.4 s¹³.

2.2.4 Analytical Crystallization Elution Fractionation

Crystallization Elution Fractionation (Supplementary Note 3, figure S4) (CEF) was created by combining the separation power achieved in the crystallization cycle (in CRYSTAF), with that obtained in the elution cycle (in TREF). The dynamic mode used during the crystallization step enable a rapid separation and better resolution than TREF and CRYSTAF²⁹.

A mass of 4 mg of each PEs was dissolved in 8 ml of 1,2,4-trichlorobenzene (TCB) at 160°C for 1 hour. After the dissolution period, the samples were loaded to the injection loop (200 µL) and injected into the CEF column using an isocratic pump. Samples were separated based on their crystallization capacity using two temperature cycles. During the crystallization step, the column temperature was lowered to 35°C, at a rate of 2°C min⁻¹, under a continuous flow of TCB (0.05 mL min⁻¹). In the elution step, the separated fractions were progressively solubilized as the temperature was increased to 130°C, at a rate of 4°C/min, under a continuous flow of TCB (1 mL/min).

An infrared detector was used to measure the concentration of eluted fractions to obtain the CEF profile and to calculate the amount of CH₃/1000C. Thus, the elution temperature was directly related to the number of short-chain branches/1000 carbon atoms by a linear relationship.

2.2.5 Differential Scanning Calorimetry

DSC experiments were carried out using TA instruments Q20 instrument to study the influence of the different molecular architecture of PEs on crystallinity. A polymer mass of 5-6 mg was weighted and prepared in a low-mass pan. Then, a temperature program was set in which the samples were first heated from -80 to 200°C, then cooled to -80 °C followed by a second heating scan to 200 °C at a heating/cooling rate of 10 °C/min under a nitrogen atmosphere. The melting temperature (T_m) was noted, as the maximum of the melting peak was determined

from both the second heating scan. The crystallization temperature (T_c) was taken from the maximum of the exothermal peak in the cooling scan. Polymer crystallinity was calculated according to the following equation. The ΔH_m^∞ used for PEs was 289 KJ/Kg³⁰.

$$X_C = \frac{\Delta H_m}{\Delta H_m^\infty} \times 100 \quad (7)$$

Where X_C is a percentage of crystallinity of the samples.

3. Results and Discussions

3.1 Polyethylene Microstructural Characterization

3.1.1 Estimation of branching content using SEC

The average molecular weight (M_w), dispersity, and the amount of LCB per molecule of each PEs chosen in this project were measured by SEC coupled with LALS and viscometer. The results are shown in Figure and the corresponding M_w , M_n , dispersity index, and the number of LCB/1000 are listed in Table 2. The LLDPEs selected for this study are ethylene1-hexene copolymers, where the LLDPE (LL2) was prepared by the use of a metallocene catalyst while the LLDPE (LL1) was synthesized with a Zeigler-Natta catalyst. In addition, both LDPEs were obtained by high-pressure free radical polymerization and are expected to contain both long and short-chain branching.

According to the literature, the LLDPEs prepared by the use of metallocene (single-site catalyst) should lead to a narrower dispersity ranging from 2 to 2.5. This is in good agreement with our results for LL2 which \mathcal{D} is close to 2, as shown in Figure . In contrast, a broad dispersity ($\mathcal{D} = 5$) was obtained for LLDE (LL1) prepared by Ziegler-Natta (Z-N) catalysis involving a multiplicity of active-sites.

The branched LDPEs present broader distributions with a higher poly dispersity index ranging from 7 to 9. The reason for this high dispersity is related to the complex LDPE molecular structure, which is formed via a free-radical

polymerization and at high pressure³¹. Therefore, the most remarkable feature of the distributions is the distinct high molecular weight tail of L1 in comparison with the others.

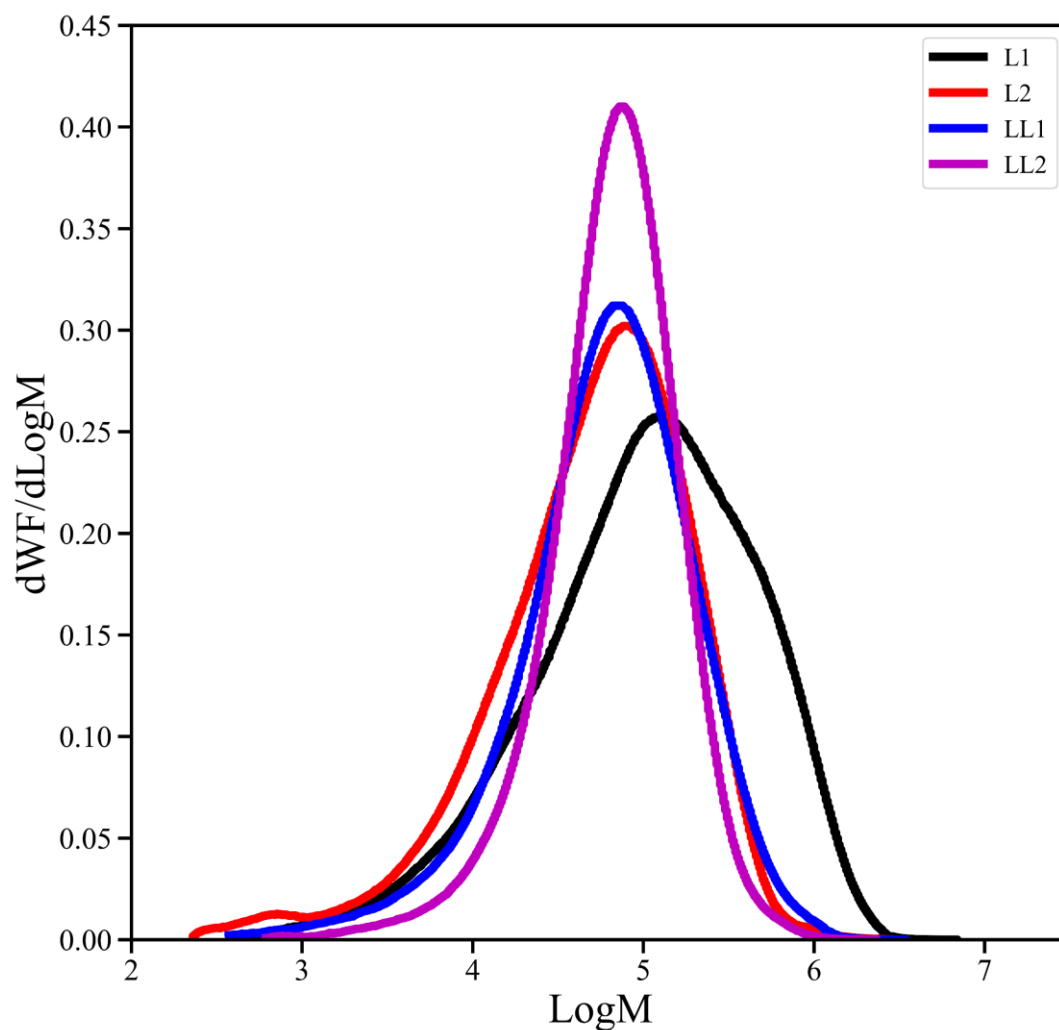


Figure 2 SEC molecular weight distributions of the 4 investigated PEs

Table 2 SEC molecular weight characteristics of the 4 investigated polymers

| Sample | M_w (g mol ⁻¹) | M_n (g mol ⁻¹) | \bar{D} | LCB/1000 C |
|--------|---------------------------------|---------------------------------|-----------|---------------|
|--------|---------------------------------|---------------------------------|-----------|---------------|

| | | | | |
|--------------------|---------|--------|-----|-----|
| LDPE (L1) | 238 600 | 26 600 | 9 | 2 |
| LDPE (L2) | 95 700 | 13 660 | 7 | 1.5 |
| LLDPE (LL1) | 107 600 | 22 900 | 5 | 0.7 |
| LLDPE (LL2) | 93 750 | 37 300 | 2.5 | 0.9 |

The amounts of LCB/1000C for each of the four types of PEs were also determined by SEC-LALS, and they are listed in Table 2. As expected, both LDPEs contain a higher amount of LCB/1000C compared to LLDPEs with values higher than 1.5 for LDPEs and less than 1 in the case of LLDPEs, respectively³².

3.1.2 Estimation of branching content by ¹³C-NMR

Qualitative analyses of chain branching in LDPEs and LLDPEs were carried out by ¹³C NMR spectroscopy using Randal methods (Supplementary Note 4). It was therefore confirmed that the LLDPEs used in this study were obtained by ethylene-1-hexene copolymerization while the structures of the LDPE polymers were a quite complex combination of short-chain branching (SCB) and long-chain branching (LCB). The identities of the short-chain branches of both LDPEs and LLDPEs are listed in Table 3. It can be seen that LL1 contains a significantly higher amount of short-chain butyl branches compared to LL2, with a value of 18/1000C against 12/1000C for LL2. These differences are directly related to the polymerization process, which means that the LL1 obtained using the Zeigler-Natta catalyst exhibits broader dispersity and, in consequence, a higher amount of short-chain butyl branching content. Otherwise, the LL2 obtained using the metallocene catalyst presents narrow dispersity and, as a result, a lower amount of short-chain butyl.

In the case of L2, both methyl and propyl branches are absent, which is common in low-density polyethylene. Moreover, for L1, the presence of methyl

branches can be explained by the insertion of a propylene monomer as a chain transfer agent to regulate both crystallinity and molecular weight.

The amounts of long-chain branches per 1000 carbon atoms determined by ^{13}C NMR are also presented in Table 3. It is around to 0.5 for both LLDPEs and 2 for both LDPEs. It is important to note that the long-chain branch content in our NMR investigation can be overestimated, as the 3Bn signal used for calculations for branches with 6 carbons or more overlap with the 3S resonance of main chain ends.

Table 3 Chain branches evidenced in the 4 investigated PEs and their content estimation by ^{13}C NMR spectroscopy

| | L1 | L2 | LL1 | LL2 |
|--|----|----|------|------|
| B1/1000C | 2 | 0 | 0 | 0 |
| B2/1000C | 1 | 1 | 0 | 0 |
| B4/1000C | 6 | 6 | 18 | 12 |
| B5/1000C | 2 | 2 | 0 | 0 |
| $B_{n \geq 6}$ /1000C | 2 | 2 | 0.6 | 0.5 |
| SCB/1000C | 11 | 9 | 18 | 12 |
| LCB /1000C | 2 | 2 | 0.6 | 0.5 |
| Total amount of chain branching /per 1000C | 13 | 11 | 18.4 | 12.5 |

3.1.3 Estimation of branching content and distribution with CEF

Crystallization Elution Fractionation (CEF) was used as a complementary tool to ^{13}C -NMR and SEC to investigate the chemical composition distribution (CCD) of both LDPEs and LLDPEs. These samples were eluted and fractionated according to their crystallization temperature. First, the chains with less

crystallinity (more SCB) were eluted, followed by the chains with higher crystallinity (less SCB). Figure 3 and 4 shows CCD of ethylene-1-hexene copolymers as measured by CEF, and the results are summarized in **Error! Reference source not found.** The CEF profiles of the studied polymers revealed distinct peaks, with the first peak (F1) is corresponding to the amorphous phase with extremely branched chains. The second and third peaks (F2 and F3) correspond to the crystalline phase of the polymer with relatively few branched chains. The sum of these peak areas gives the average total branching content expressed per thousand carbon atoms (/1000C) and is also listed in the Table 4. Notably, the branching in LDPE is referred to as long-chain branching (LCB), whereas the branching in LLDPE is referred to as short-chain branching (SCB)³³.

As shown in Figure 3, both LDPEs display unimodal branching distribution showing one peak in the crystalline phase (F2) and a narrow CEF profile with a total branching content of 19 for L1 and 14 for L2, consistent with a free-radical polymerization mechanism. While, as shown in Figure 4, both LLDPEs exhibit a bimodal branching distribution, showing two peaks in the crystalline phase (F2 and F3). The LL1 has a very broad branching distribution and a less uniform composition distribution (distance between F2 and F3 in Figure) with a total branching content of 22. This behavior is expected from the Ziegler-Natta catalyst, since there are more active sites used to generate PE chains with varying comonomer compositions and chain lengths. Contrarily, the LL2 has a more uniform microstructure with narrow CCDs and a total branching content of 13, which may be ascribed to the presence of only one active site in metallocene catalysts. The single-site catalyst (metallocene catalysts) technology is used to tailor the molecular architecture of polyolefin demands by adjusting catalyst structures and process parameters. The well-controlled microstructures could be employed to help design polymerization models. These results are in agreement with other authors.

To summarize, the CEF analysis was used to obtain information about the branching distribution of the studied PEs that the ^{13}C NMR method alone cannot provide. As evidenced in table 3, 4 and 5, the CEF findings were in the same order of magnitude as those obtained using the ^{13}C -NMR analysis, indicating the reliability of both methods. Interestingly, the CEF method does not efficiently fractionate LCB existing in the PEs, since the LCB behave like the main chains and thus have some impacts on chain crystallinity. On this basis, only findings determined by ^{13}C -NMR can be used to predict the LCB content.

Table 4 Characteristic of the PEs CEF fractions

| Sample | Peak elution temperature ($^{\circ}\text{C}$) | | | $\text{CH}_3/1000\text{C}$ |
|-------------|---|----|----|----------------------------|
| | F1 | F2 | F3 | |
| LDPE (L1) | 10 | 75 | - | 19 |
| LDPE (L2) | 11 | 81 | - | 14 |
| LLDPE (LL1) | 10 | 66 | 94 | 22 |
| LLDPE (LL2) | 11 | 78 | 82 | 13 |

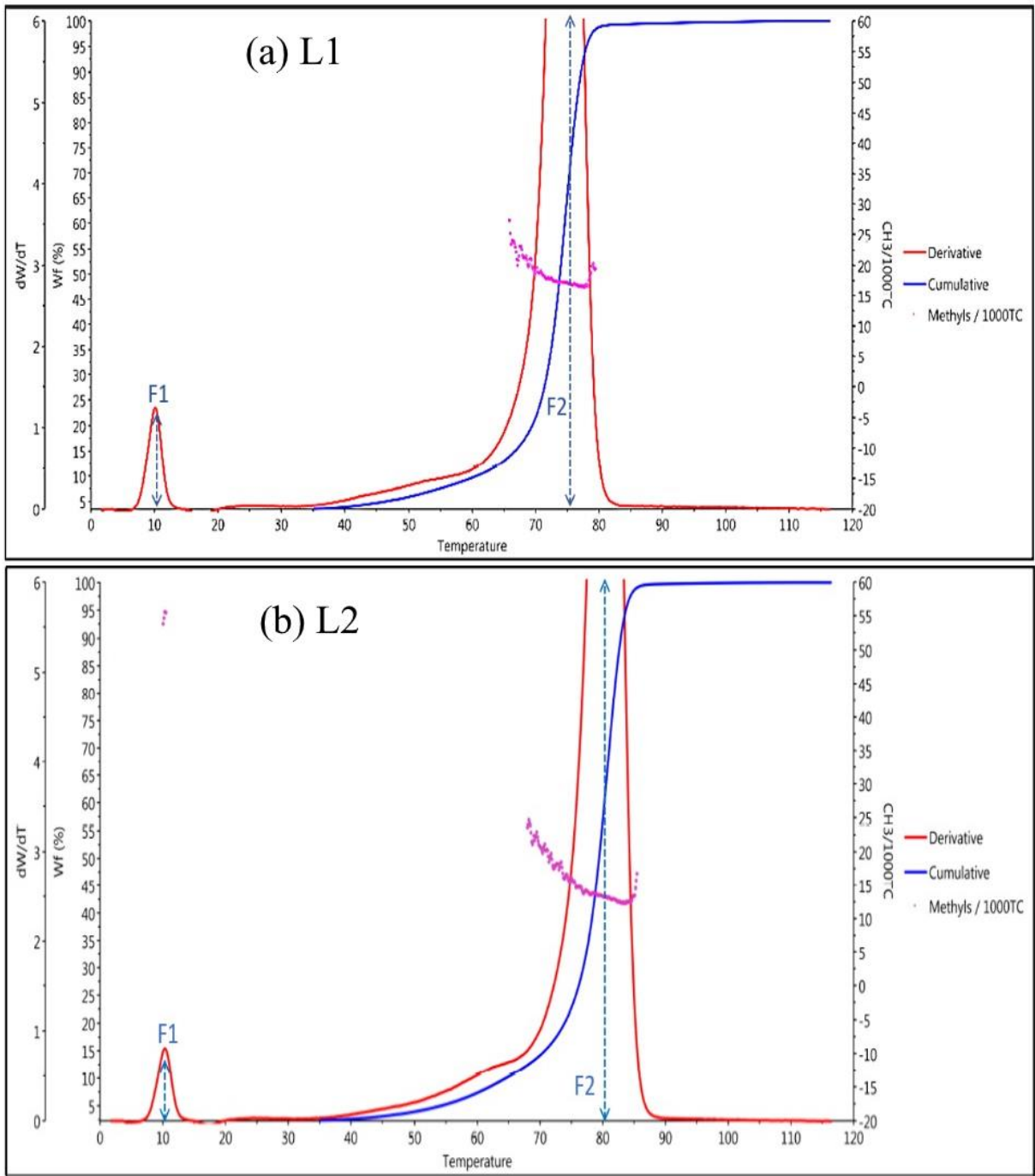


Figure 3 CEF profiles of LDPEs produced by free radical polymerization.

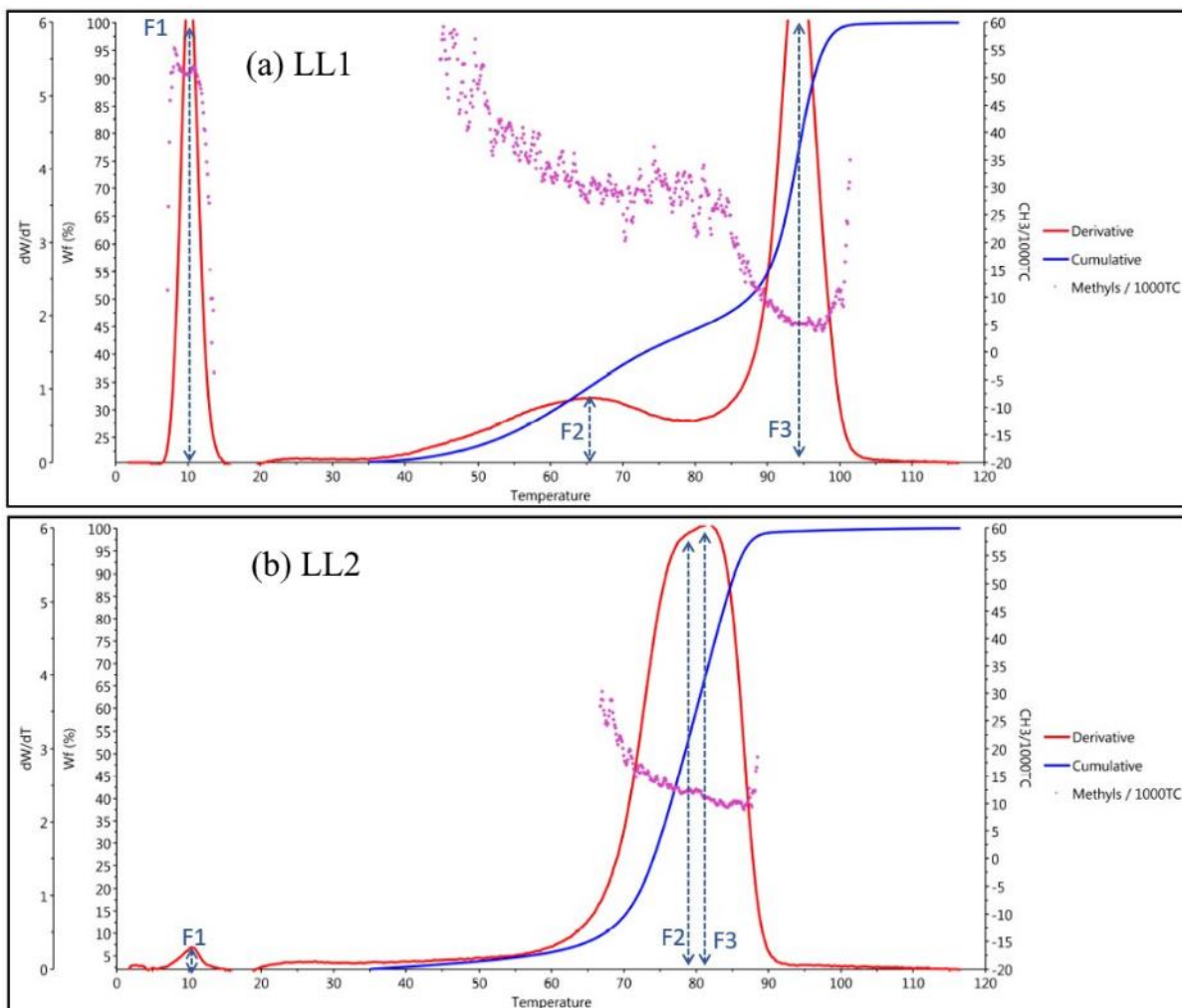


Figure 4 Effect of catalyst type of ethylene/1-hexene copolymers determined by CEF: LL1 obtained using Z-N catalyst (a) and LL2 obtained metallocene catalyst (b).

Table 5 summarize the calculated LCB/1000C with the two methods. The obtained results with SEC, ¹³C NMR and CEF highlighting the accuracy of our procedures. Comparison between different methods to measure

| Sample | SEC LCB/1000C | ¹³ C NMR C _n (n>=6)/1000C | CEF CH ₃ /1000C |
|-----------|------------------|---|-------------------------------|
| LDPE (L1) | 2 | 2 | 19 |
| LDPE (L2) | 1.5 | 2 | 14 |

| | | | |
|----------------|-----|-----|----|
| LLDPE (LL1) | 0.7 | 0.6 | 22 |
| LLDPE (LL2) | 0.9 | 0.5 | 13 |

3.1.4 Differential scanning calorimetry (DSC)

The thermal fractionation of the studied PEs was measured using DSC as shown in Figure and the detailed results are listed in Table 6. Various crystallization parameters of both sets of polyethylenes measured by DSC. It is quite clear, from the melting process, that LLDPE2 with lower branch content is rather different from all studied PEs, since having two different melting peaks of the heat flow, a larger one at 107°C and a narrower one at 118°C. This could indicate the presence of two crystalline populations.

Comparing these results with those obtained from CEF, it seems that the first melting peak that appears at lower temperature represents the short-branched fractions F2, while the second narrower peak refers to the more linear components with lower short-chain branching content F3. The formation of a double peak for LLDPE having lower branch content has also been observed by Cabrera in their previous work. In this last reference of our group, we hypothesized that the low branching content of LLDPE may result in a segmented intra-chain comonomer distribution that could initiate the segregated crystalline state. Furthermore, only one melting peak can be viewed for the others PE in their melting cycle. This single broader peak may be related to the single crystalline population. Crystallization temperatures (T_c), melting point (T_m), and the degree of crystallinity (X_c %) of the four types of polyethylene were calculated from the second heating ramp. The values obtained from the DSC curve are reported in Table 6. It can be seen that the degree of crystallinity of LL1 is much higher than

that of LL2, with values of 46% for LL1 and 35% for LL2, respectively. This trend is expected as the LL1 has a higher melting temperature. Moreover, comparing the crystallinity and the melting temperature of L1 and L2, it can be seen that they do not change significantly.

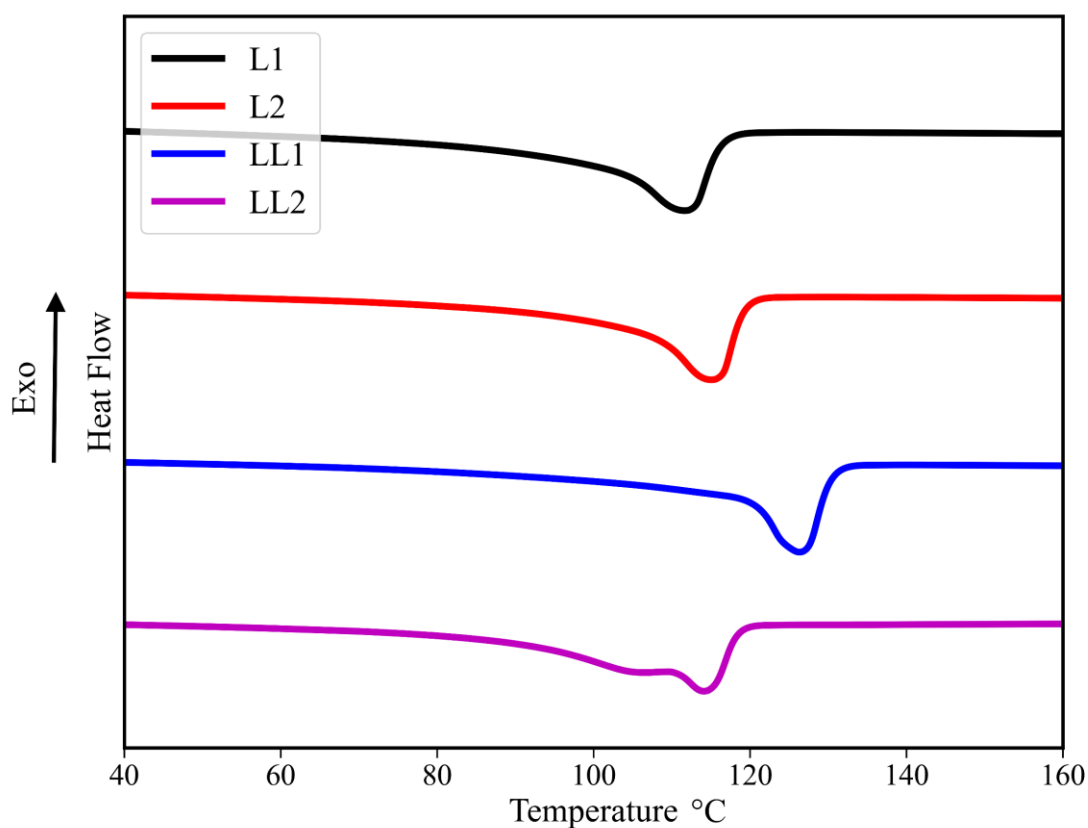


Figure 5 DSC thermograms for the different PEs

Table 6 Various crystallization parameters of both sets of polyethylenes measured by DSC

| Samples | Tc (°C) | Tm (°C) | Xc (%) |
|-----------|---------|---------|--------|
| LDPE (L1) | 93 | 112 | 42 |

| | | | |
|-------------|-----|-----------|----|
| LDPE (L2) | 98 | 115 | 38 |
| LLDPE (LL1) | 110 | 126 | 46 |
| LLDPE (LL2) | 99 | 107 - 118 | 35 |

3.2 The influence of molecular architectures of PEs on rheological properties

3.2.1 Dynamic time sweep

In this section, we examine the linear viscoelastic properties of both linear and branched PEs at different temperatures ranging from 160°C to 240°C. For the sake of clarity, only the rheological results at 190°C are presented here. Prior to testing, it was necessary to first check that the polymer melt does not degrade during the dynamic shear measurements (Small Amplitude Oscillatory Shear, SAOS). An example of the normalized viscosity and storage modulus as a function of time is shown in Figure at a reference temperature of 190°C. First, it can be seen that the viscoelastic responses for both LLDPEs, don'ts o change over the testing time. This suggests that the molecular structure of the LLDPEs remained relatively unchanged³⁴. Likewise, at a shorter time, the thermal stable behavior of the LDPE plots is highlighted, whereas at a longer time ($t > 15$ min), the behavior of the LDPEs is different compared with the linear one. A vertical shift was required at a longer time, which could be due to some crosslinking among the LDPE chains or degradation mechanisms occurring over a long period time.

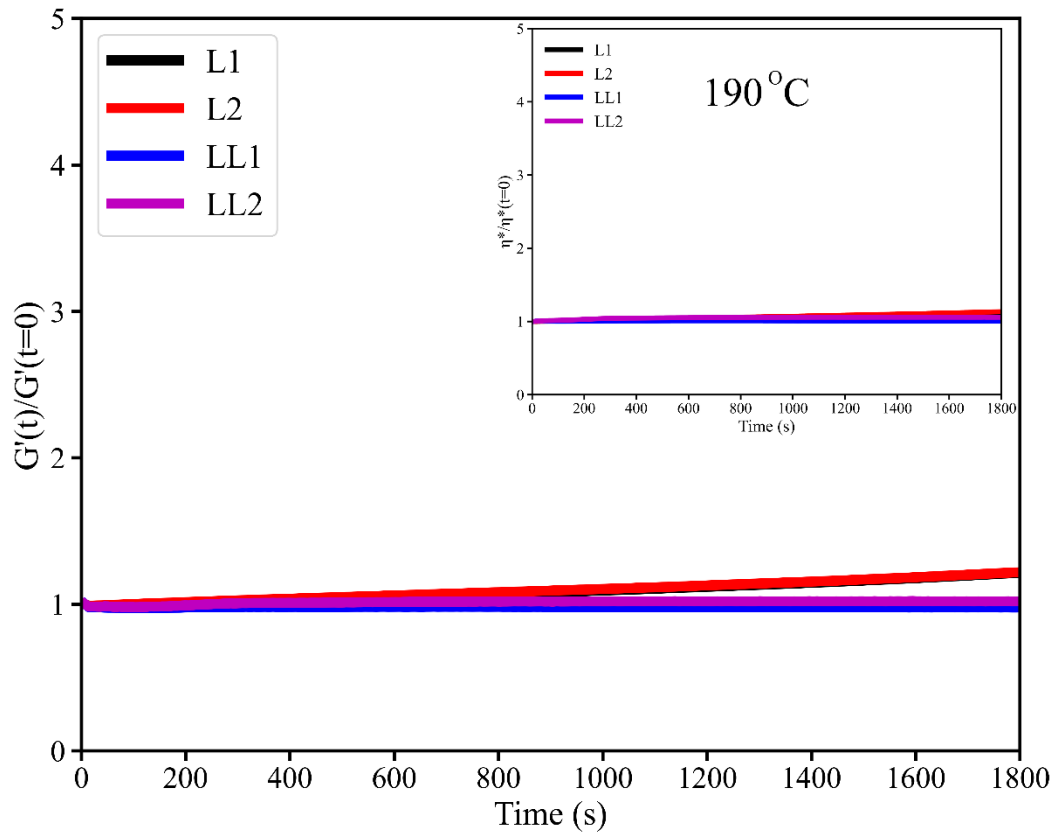


Figure 6 Evolution comparison of $G'/G'(t = 0)$ and $\eta^*/\eta^*(t=0)$ as a function of healing time at 190°C with an angular frequency of 0.1 rad/s for neat PEs.

3.2.2 Dynamic frequency sweep

The viscoelastic properties of polymeric materials are very sensitive to the molecular structure of polyethylene including short/long chain branching and dispersity. Figure Depicts the dynamic complex viscosity (η^*) against angular frequency (ω) for all the neat polymers at a reference temperature of 190°C.

Firstly, it can be observed that the rheological behavior of both linear and branched PEs are different with some shear-thinning behaviors, which are more pronounced beyond 10 rad/s. Their zero-shear viscosity can be simply deduced as the $\lim_{\omega \rightarrow 0} \eta^* = \eta_0$ in the Newtonian regime, except for LDPEs the zero-shear viscosity values were not reached experimentally. As found in the literature, the presence

of long-chain branching causes a significant increase in shear-frequency/thinning behavior³⁵.

Moreover, it can be clearly seen that LDPEs are more viscous comparing to the linear ones at lower frequency regions. This behavior was expected since the LDPE contains a high amount of LCB/1000C compared to LLDPE with values of 2 for LDPEs and close 0,5 for LLDPEs, respectively. The presence of long-chain branching created more entanglements thus resulting in higher molecular weights as well as rising viscosities at lower frequencies and significant shear thinning at higher frequencies³⁶. Herein, the zero-shear viscosity (η_0) was calculated by fitting the experimental data with the Carreau-Yasuda model [1] and then compared with the calculated viscosity.

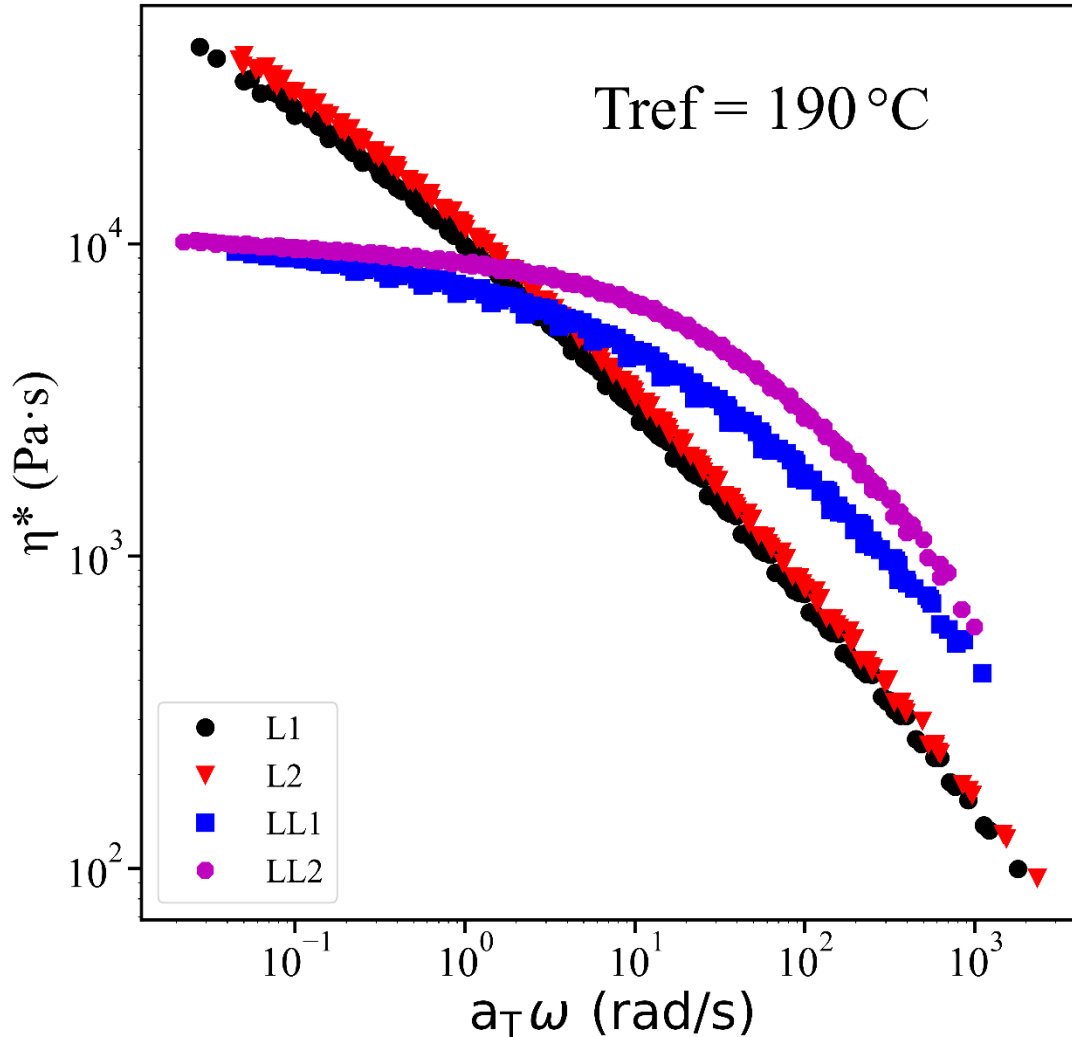


Figure 7 Master curve of complex viscosity versus angular frequency (shear rate) at a reference temperature of 190°C for all PEs.

Master curves of storage modulus (G') and loss modulus (G'') reduced at a reference temperature of 190°C for all neat PEs are given in Figure . The rheology at the terminal zone was found to follow the standard relations $G' \sim \omega^2$, $G'' \sim \omega^1$ for the neat polymers. The crossover of G' and G'' allow us to calculate the relaxation time ($\tau_d = \eta_0 / G_N^0$) The main characteristics of the selected PEs are

summarized in Table 7. The plateau modulus (G_N^0) was estimated with van Gurp-Palmen plots by extrapolation at the lower limit of δ .

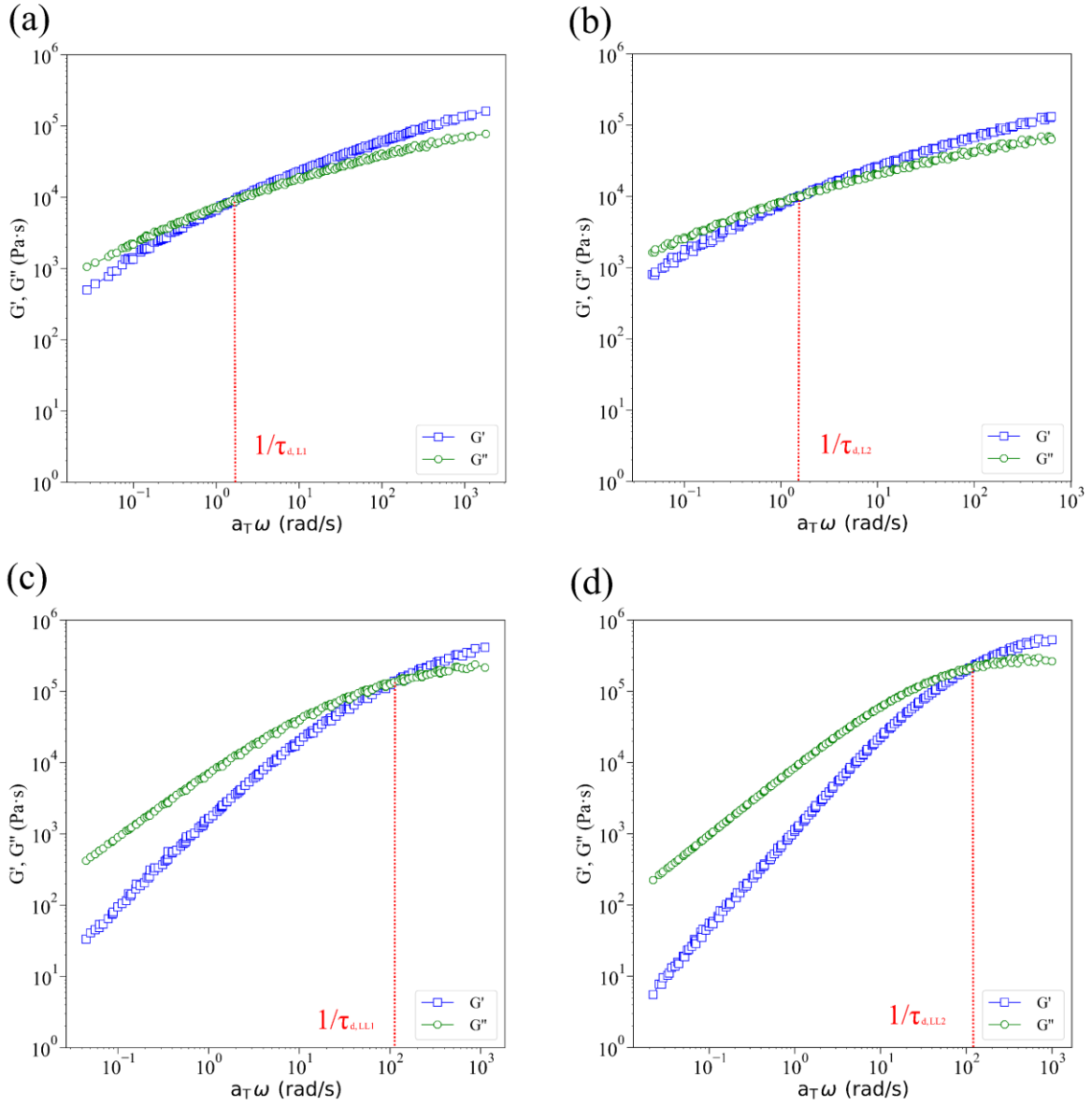


Figure 8 Master curves of storage modulus (G') and loss modulus (G'') reduced at a reference temperature of 190°C for all PEs.

The number of entanglements per chain (Z) can be evaluated as $Z=M_w/M_e$. The weighted average terminal relaxation time determined from the cole-cole plots ($\eta''\sim\eta'$) was taken as the order of reptation time (τ_{rep}). Furthermore, the critical molecular weight M_c is to be twice M_e ³⁷. The latter is calculated according to $G_N^0=\rho RT/M_e$ with the melt mass density (ρ) and gas constant (R).

Additionally, the Rouse relaxation time might be calculated using the following equation: Additionally, the Rouse relaxation time might be calculated using the following equation (8):

$$\tau_R = \frac{6M_w \eta_0}{\pi^2 \rho RT} \left(\frac{M_c}{M_w} \right)^{2.4} \quad (8)$$

Table 7 Material characteristics based on linear viscoelastic measurements at 190 °C

| Sample code | L1 | L2 | LL1 | LL2 |
|--------------------------------------|--------|-------|--------|-------|
| Mw(g/mol) | 238600 | 95700 | 107600 | 93750 |
| D | 9 | 7 | 5 | 2,5 |
| LCB/1000C (¹³ C NMR) | 2 | 2 | 0,6 | 0,5 |
| SCB/1000C (¹³ C NMR) | 11 | 9 | 18 | 12 |
| η_0 (carreau) (Pa.s) | 35169 | 13785 | 7619 | 9232 |
| Measured η^* (0,01rad/s) (Pa.s) | 38459 | 16426 | 8280 | 9845 |
| Ea (KJ/mol) | 53 | 51 | 26 | 31 |
| G_N^0 (x105Pa) | 1,1 | 1 | 2,6 | 6 |
| Me (kg/mol) | 32,5 | 36.5 | 14 | 6 |
| Mc (kg/mol) | 65 | 73 | 28 | 12 |
| Z | 7 | 3 | 8 | 16 |
| τ_m (s) | 6.3 | 3.14 | 0.06 | 0.06 |
| τ_R (s) | 0.1 | 0.1 | 0.005 | 0.001 |

The activation energy of the viscous flow (Ea) of the selected PEs was obtained from the $\log \eta_0$ plotted versus $1/T$ within a temperature range of $160^\circ\text{C} < T < 240^\circ\text{C}$. Obviously, it can be seen from Table that the activation energy of each LDPEs is higher compared to that of LLDPEs. The corresponding values for the two LDPEs

are around 50KJ/mol, typical for LDPEs^{34,38}. This is due to the long-chain branches that are obtained using a free-radical mechanism. On contrary, the flow activation energy values of LLDPEs are 26 KJ/mol for LL1 and 31KJ/mol for LL2, respectively, values again typical for LLDPEs ³⁹. This is related to the negligible long chain branching in LLDPE.

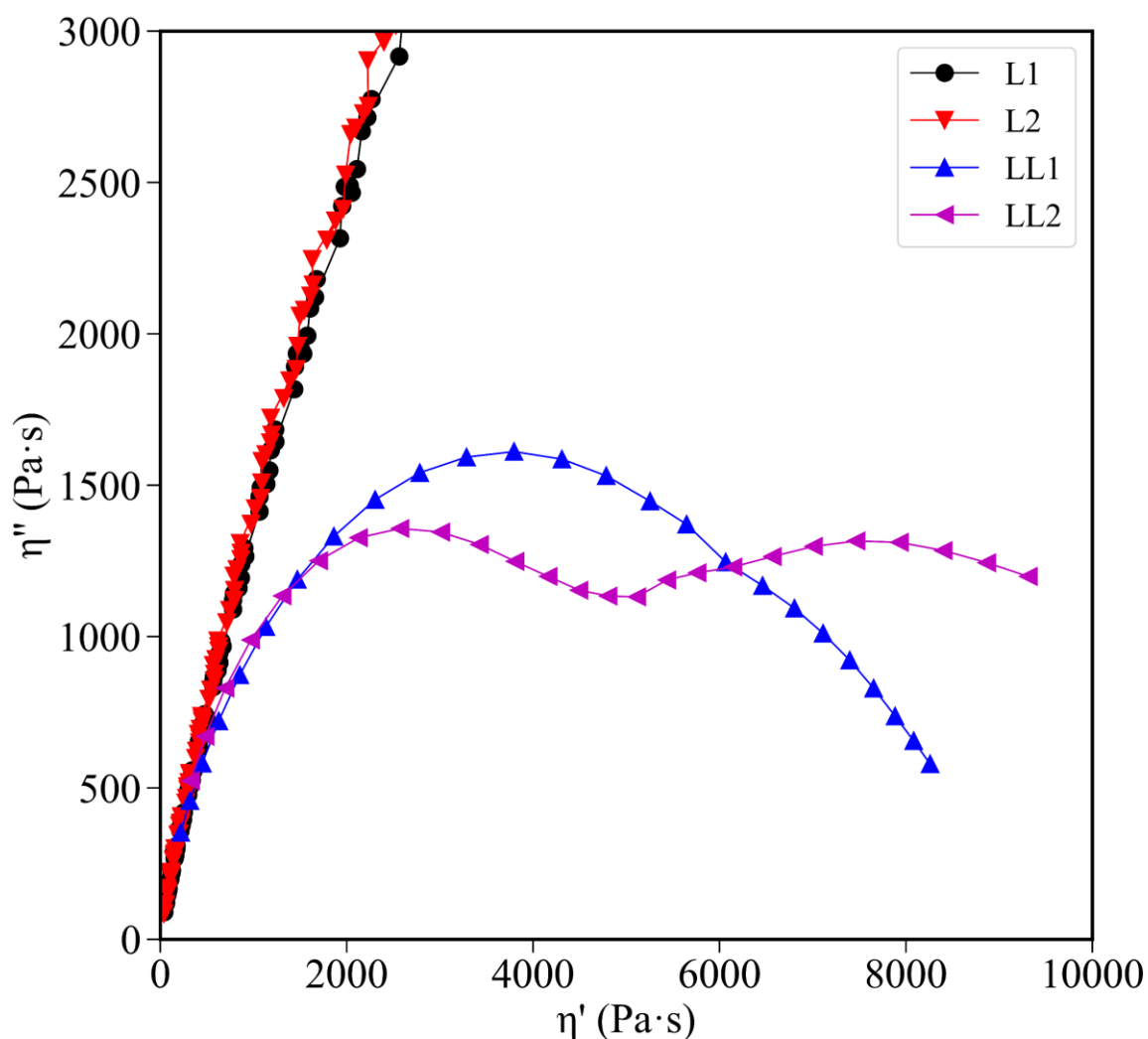


Figure 9 Cole-cole plots for neat PEs at 190°C

Figure presents the plots of η'' versus η' , which are typical Cole-Cole plots. The LDPEs display an interesting window to check the effect of their long relaxation process in comparison respectively to linear LLDPEs. A semicircular

shape was obtained for LL1 with a relaxation time of 0.25s. For LLDPE2 we note the presence of two prominent relaxations peaks. The first, at shorter times (0,04s), was related to the relaxation of the short-chain while the second one, situated at (16s), could be attributed to the reptation of the backbone. The intensity of the weighted relaxation peak of LL2 is a little weaker which means the elasticity is reduced due to the lower molecular weight. The wide relaxation peak of LL1 indicates a non-uniform chain structure. However, for LDPEs, no arc shape was seen even at low frequencies indicating a very long relaxation time for this kind of polymer. These differences can be explained by the different PEs structures and molecular weight distribution. The presence of LCB has a more pronounced effect on viscoelastic properties.

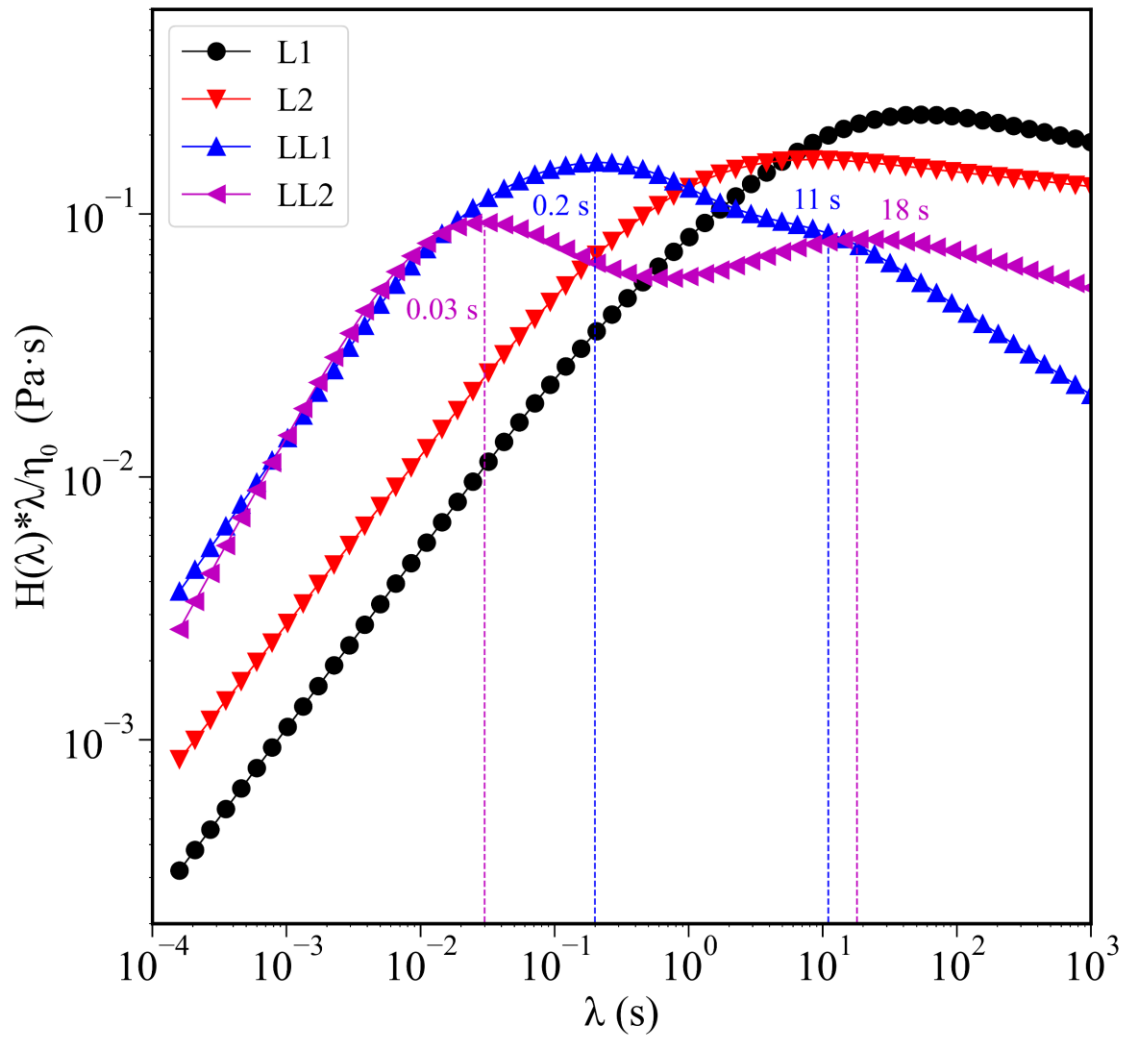


Figure 10 Weighted relaxation spectra of the PEs at 190°C.

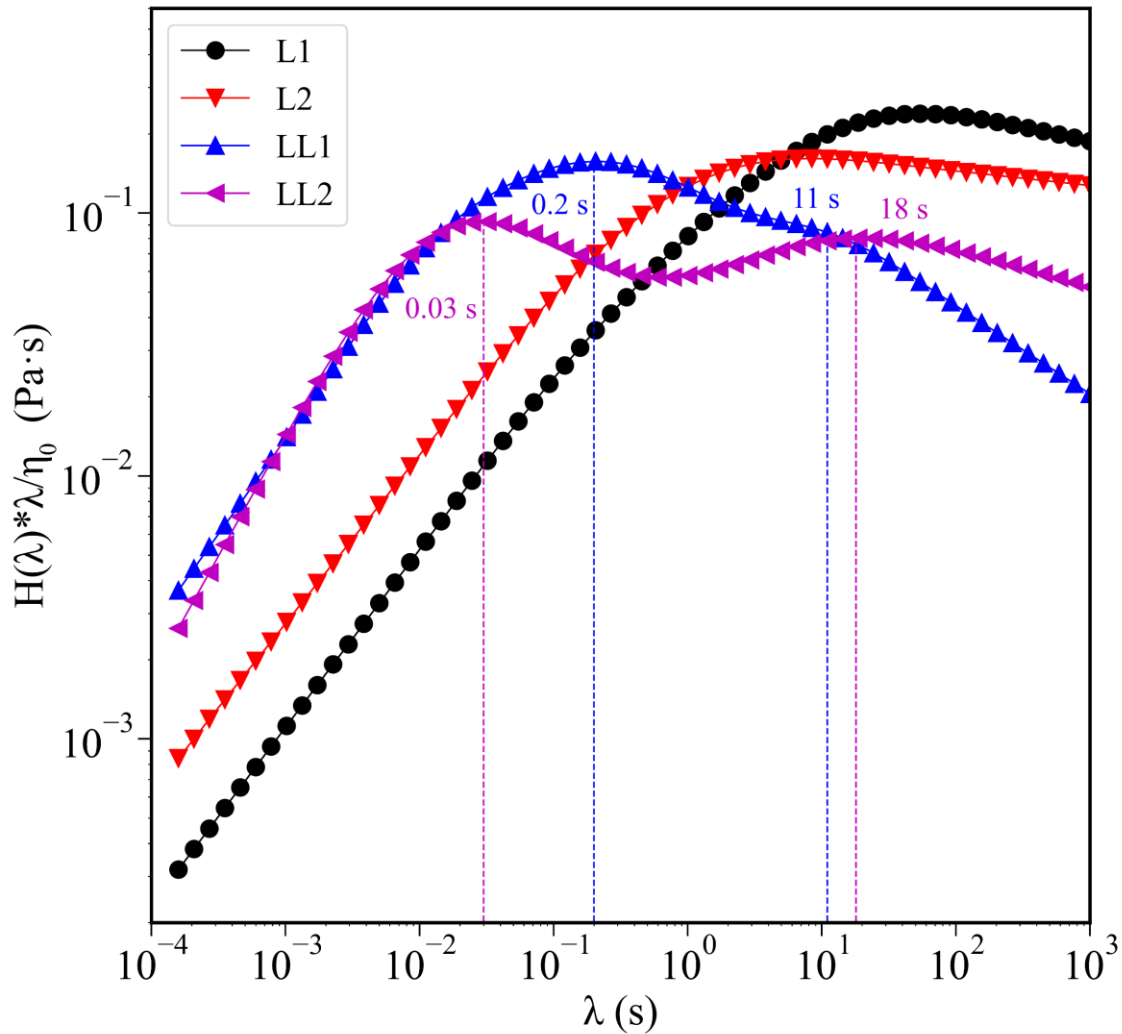


Figure illustrates the weighted relaxation spectra normalized by the zero-shear viscosity as a function of the relaxation time of neat polymers at 190°C. They are normalized to eliminate the effect of viscosity mismatches between polymers. This reflects the continuous time distribution of chain relaxations. The relaxation spectrum was determined using the dynamic modulus. As depicted in the same Figure 9, the PEs show different characteristic relaxation times because of their different structures and molecular weight distributions.

For LLDPEs, two prominent relaxation spectrum peaks could be clearly observed at about 0.03s and 18s for LL2. In addition, the relaxation times of LL1

are located at 0.2s and 11s. The first peak corresponding to the relaxation of short chains is due to the reptation of the linear chains (backbone). The second one is related to the existence of a second phase with a longer relaxation time.

While for LDPEs the relaxation spectrum could not be detected in the present experimentally available range of frequency, LCB suppresses reptation time and cause a much slower chain relaxation. These results are in agreement with Cole-cole plot Figure .

The relaxation time of LLDPE is dominated by the reptation of long chains, hence this explains why the rheological properties of a polymer are strongly influenced by the longest chains in the system.

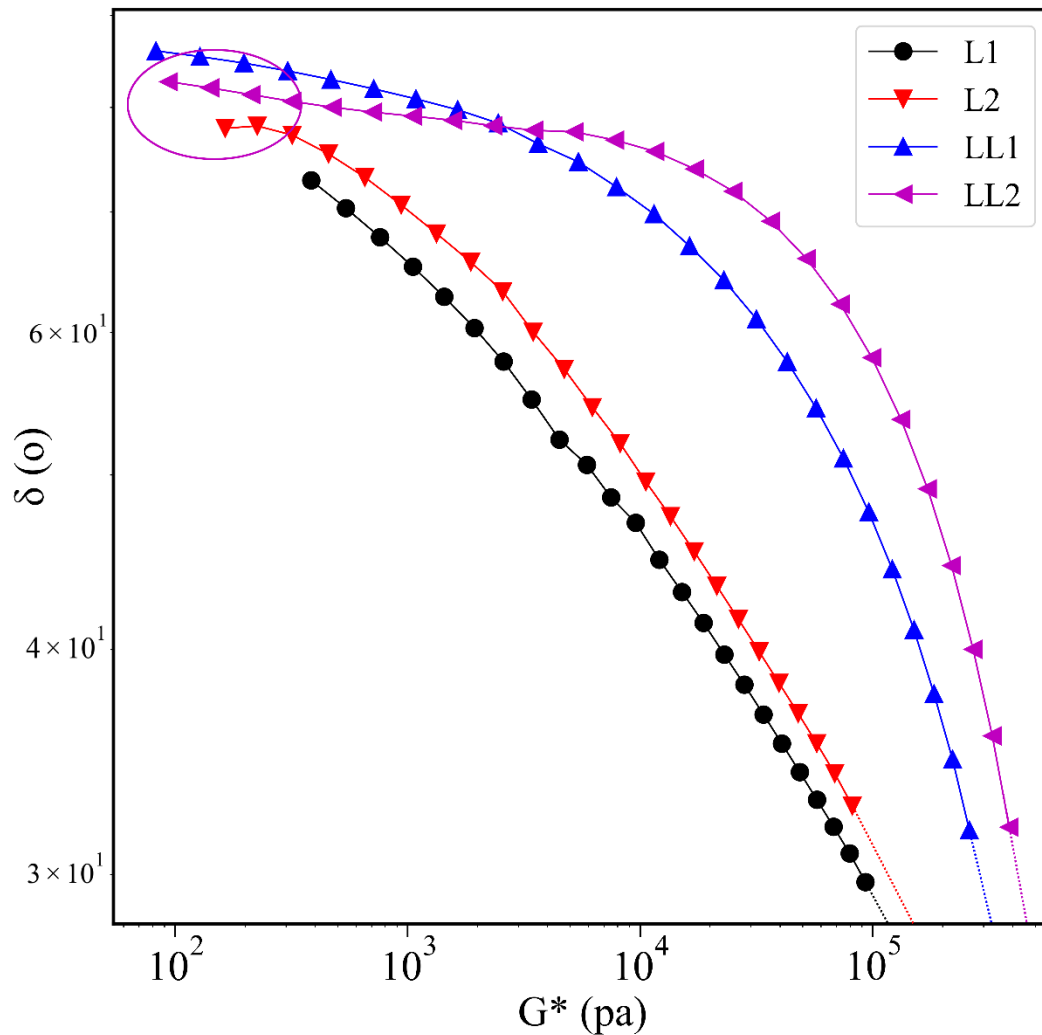


Figure 11 Van Gorp-Palmen (vGP) plots of phase angle (δ) versus complex modulus (G^*) for all linear and branched PEs at 190°C.

Figure depicts the Van Gorp-Palmen plots of these PEs at 190°C. The plots show the evolution of the phase angle in terms of $|G^*|$ for all linear and branched PEs. G_N^0 was estimated by an extrapolation of these curves at the lower limit of δ . The phase angles are strongly dependent on molecular weight and are very sensitive to polydispersity and the presence of long-chain branching. As the number of LCBs increases, the entire curve shifts to the left of the complex

modulus axis. We note that the effect of LCB is similar to that of polydispersity. To sum, the LDPEs display high elastic behaviors than LLDPE polymers.

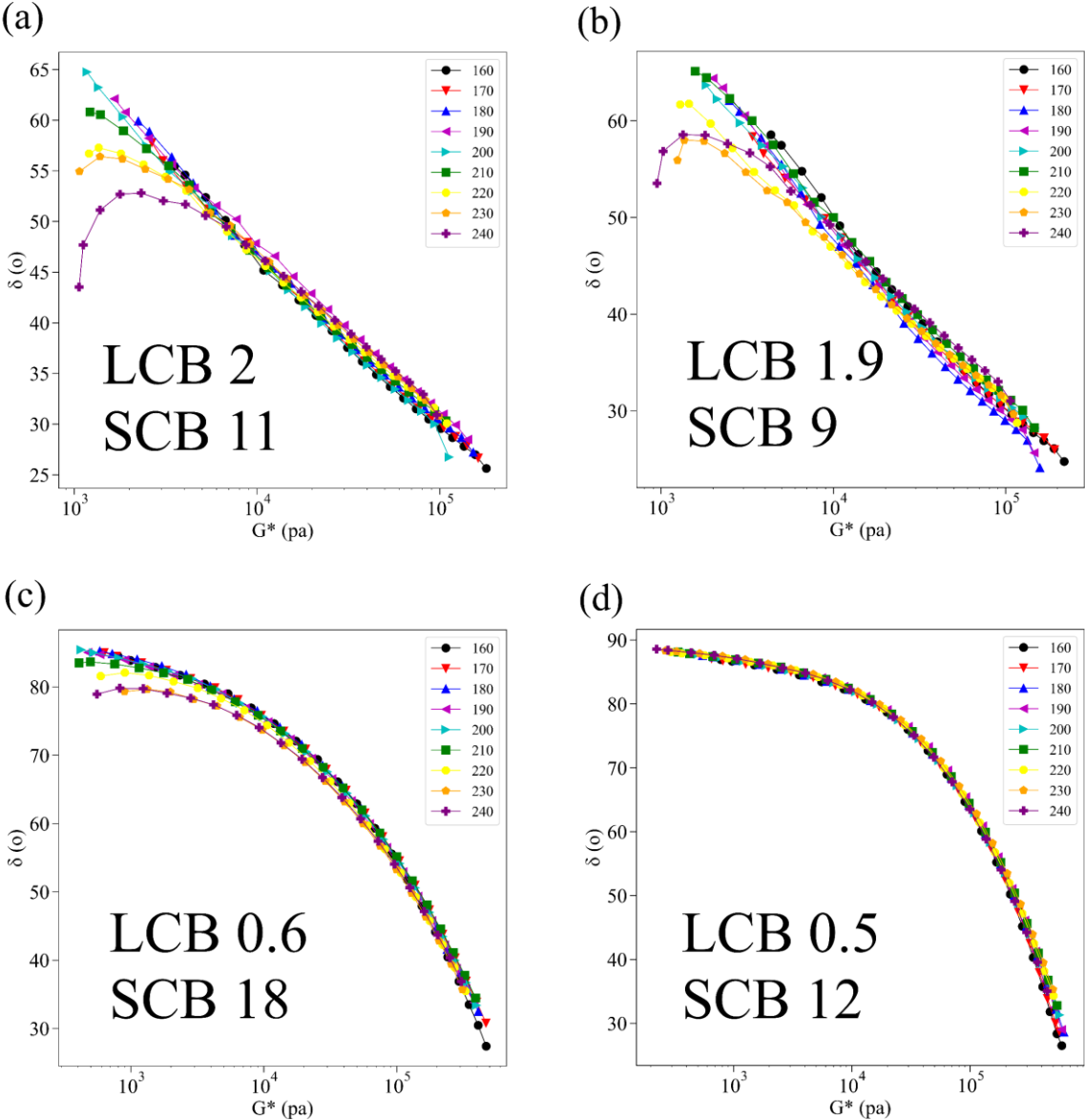


Figure 11 Representative vGP curves of linear and short-chain branched PE over the temperature range from 160 °C to 240°C.

Figure shows the thermal-rheological behavior found for LLDPEs and LDPEs in terms of a δ - $|G^*|$ plot. The LLDPE metallocene ethylene-hexene copolymers with very low levels of long-chain branching are thermal-rheologically simple,

i.e., the superposition appears to be good. We conclude that these linear copolymers exhibit only mild complexity. While long-chain branching results do not exhibit time-temperature superstability, they are thermal-rheologically complex.

3.2.3 Extensional rheology of all PEs at 190°C

Uniaxial extensional rheology was used to investigate the melt flow properties of the four different types of polyethylene and to determine their processability under flow conditions simulating the coextrusion system. Figure shows the evolution of extensional viscosity as a function of time at 190°C with extension rates varying from 0.1 to 10 s⁻¹. The transient extensional viscosities of neat polymers agree well with the LVE envelope. The latter was determined independently from linear viscoelastic shear rheology measurements and plotted as a dashed black line. L1 seems to show the strongest strain-hardening among the tested polyethylene's. This observed behavior is expected since this polymer contains broader dispersity, molecular weight distribution and also a high amount of long-chain branching. The numbers of LCB per 1000 monomers were found to be 2 for LDPE, which favored the entanglement between chains. S.L. As explained by S. Lindeblad ⁴⁰, the origin of the strain hardening behavior was attributed to the number of branches that increase the monomeric friction between a small molecule and its surrounding ones, allowing the backbone to be extended more than its linear polymer. Consequently, as the arms with the remainder of the molecule are sufficiently aligned by the elongational flow, the friction reduces, and the polymer backbone contracts with a less stretched configuration, obtaining the steady-state stress. Similar behavior was seen in L2 and it could be correlated again to the amount of short and long-chain branching as we have demonstrated previously.

Therefore, in terms of LL2, a positive deviation in extensional viscosity from the LVE envelope at larger strains was observed, indicating an enhanced strain hardening. This result was not expected since this polymer has narrower dispersity,

lower molecular weight, and negligible long chain branching LCB (0.5 LCB/1000C). It can be said that extensional rheology is extremely sensitive to even trace amounts of LCB. Whereas this hypothesis doesn't seem to be valid for the other LL. These results are in correlation with the literature indicating that even a small amount of LCB may result in significant differences in the rheological behavior^{40,41}. A HMMSF model was used to predict the extensional rheology behavior and compared with the experimental data which can be found in supplementary information ()

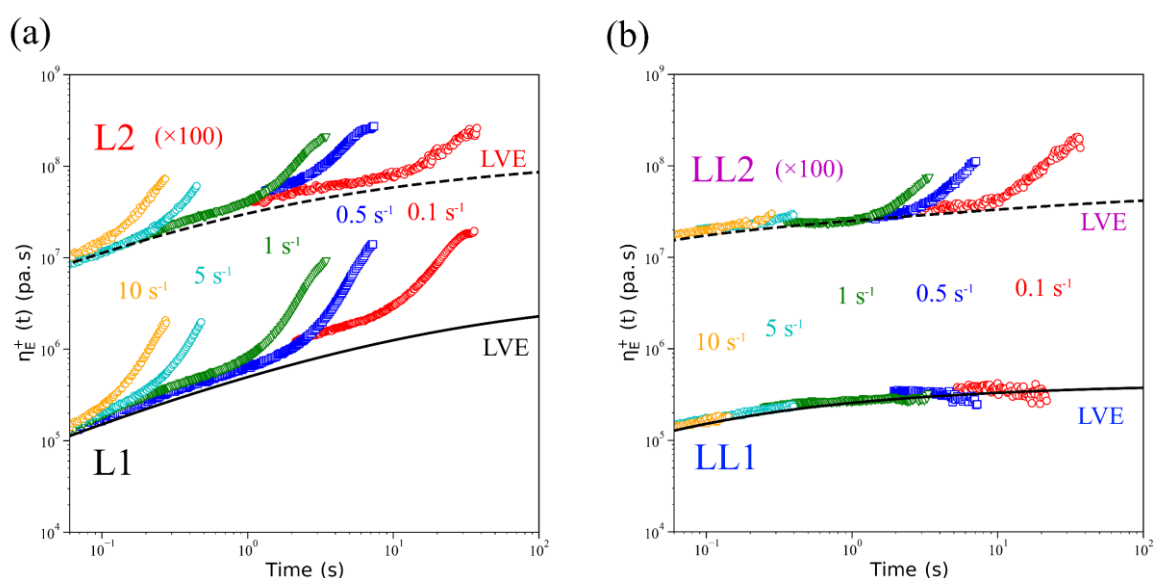


Figure 13 Extensional viscosity at the temperature of 190°C with the extensional rate varying from 0.1 to 10 s⁻¹ for the different PEs. The black lines represent the LVE envelope (i.e., 3η₀⁺(t)) determined from shear measurement.

4. Conclusion

The physicochemical, thermal, and rheological properties for the four kinds of polyethylenes composed by LDPEs and LLDPEs were studied. It was found by SEC and ¹³CNMR that LDPEs contain high molecular weight and a great amount

of LCB in comparison with linear ones, which is in good agreement with the dispersity of each sample. The reason for this difference is related to the complex LDPE molecular structure, which is formed via a free-radical polymerization. CEF test were conducted as a complementary tool for ^{13}C NMR and SEC to investigate the chemical composition distribution (CCD) of the studied PEs. The findings indicated that the CCD of each sample depends strongly on the catalyst used. The LL1 produced by Z-N catalyst exhibit broad branching distribution and less uniform composition distribution, whereas the LLDPE2 obtained by metallocene catalyst show more uniform microstructure with narrow chemical composition distributions. Unlikely, the two LDPEs display wide and unimodal distribution, as expected from the free-radical polymerization mechanism used to fabricated it. Moreover, the CEF findings were in the same order of magnitude as those obtained using the ^{13}C NMR analysis, indicating the reliability of both methods. Additionally, the thermal behavior of branched and linear PEs was correlated to its microstructural parameters. All samples display unimodal crystallization profiles except the LLDPE produced by Metallocene catalyst with two complex endotherm peaks revealing heterogeneous intra-chain and inter-molecular SCB distributions. Furthermore, the rheological results were strongly influenced by the presence of LCB. It was found that LDPEs with a higher amount of LCB (2 LCB/1000C), and broad MWD exhibited higher zero shear-viscosity, higher values of storage modulus, longer relaxation times, and higher activation energy when compared to linear LLDPEs^{40,42}. Indeed, the presence of long-chain branching leads to more pronounced strain hardening behavior in the elongational flow which is neglected in linear species. The molecular structure of linear and branched PEs is consistent with the rheological properties. Finally, these findings lead to a better understanding of the relationships between the molecular structure of linear and branched PEs with rheological properties.

Author's Statements

Funding information: French National Research Agency (ANR) through the NOEMR project (ANR-20-CE06-0003)

Authors contribution: Jixiang Li: drafted the manuscript, performed the rheology test; Ibtissam Touil: conceived and designed the experiments, performed the DSC test and draft editing; Carlos Fernández de Alba: performed the rheology test; Fernande Boisson: performed the NMR test and data analyzation, draft editing; Olivier Boyron: performed the SEC test and data collection, draft editing. Bo Lu: conceptualization and draft editing, Huagui Zhang: conceptualization and draft editing, Esmaeil Narimissa: performed the modelling of extensional rheology, Abderrahim Maazouz: supervision, conceptualization; Khalid Lamnawar: supervision, conceptualization and draft editing.

The authors declare no competing financial interest.

Acknowledgements

The authors are grateful for the financial support from the French National Research Agency (ANR) through the NOEMR project (ANR-20-CE06-0003) and Jixiang Li and Khalid Lamnawar thanks also CSC program for support.

References

- (1) Mangaraj, S.; Goswami, T. K.; Mahajan, P. V. Applications of Plastic Films for Modified Atmosphere Packaging of Fruits and Vegetables: A Review. *Food Engineering Reviews* **2009**, *1* (2), 133–158.
- (2) Simpson, D. M.; Vaughan, G. A. Ethylene Polymers, LLDPE. In *Encyclopedia of Polymer Science and Technology*; 2001.
- (3) Gedde, U. W.; Viebke, J.; Leijström, H.; Ifwarson, M. Long-Term Properties of Hot-Water Polyolefin Pipes—a Review. *Polymer Engineering & Science* **1994**, *34* (24), 1773–1787.
- (4) T. L. Hanley; R. P. Burford; R. J. Fleming; K. W. Barber. A General Review of Polymeric Insulation for Use in HVDC Cables. *IEEE Electrical Insulation Magazine* **2003**, *19* (1), 13–24.
- (5) Cai, L.; Peng, Y.; Xu, J.; Zhou, C.; Zhou, C.; Wu, P.; Lin, D.; Fan, S.; Cui, Y. Temperature Regulation in Colored Infrared-Transparent Polyethylene Textiles. *Joule* **2019**, *3* (6), 1478–1486.
- (6) Hsu Po-Chun; Song Alex Y.; Catrysse Peter B.; Liu Chong; Peng Yucan; Xie Jin; Fan Shanhui; Cui Yi. Radiative Human Body Cooling by Nanoporous Polyethylene Textile. *Science* **2016**, *353* (6303), 1019–1023.
- (7) van der Werff, H.; Heisserer, U. 3 - High-Performance Ballistic Fibers: Ultra-High Molecular Weight Polyethylene (UHMWPE). In *Advanced Fibrous Composite Materials for Ballistic Protection*; Chen, X., Ed.; Woodhead Publishing, 2016; pp 71–107.
- (8) Lin, Y.; Cao, J.; Zhu, M.; Bilotti, E.; Zhang, H.; Bastiaansen, C. W. M.; Peijs, T. High-Performance Transparent Laminates Based on Highly Oriented Polyethylene Films. *ACS Appl. Polym. Mater.* **2020**, *2* (6), 2458–2468.
- (9) Basko, A.; Pochivalov, K. Current State-of-the-Art in Membrane Formation from Ultra-High Molecular Weight Polyethylene. *Membranes* **2022**, *12* (11).
- (10) Agrawal, P.; Silva, M. H. A.; Cavalcanti, S. N.; Freitas, D. M. G.; Araújo, J. P.; Oliveira, A. D. B.; Mélo, T. J. A. Rheological Properties of High-Density Polyethylene/Linear Low-Density Polyethylene and High-Density Polyethylene/Low-Density Polyethylene Blends. *Polymer Bulletin*. 2021.
- (11) Wu, S.-L.; Qiao, J.; Guan, J.; Chen, H.-M.; Wang, T.; Wang, C.; Wang, Y. Nascent Disentangled UHMWPE: Origin, Synthesis, Processing, Performances and Applications. *European Polymer Journal* **2023**, *184*, 111799.
- (12) Kessner, U.; Kaschta, J.; Stadler, F. J.; Le Duff, C. S.; Drooghaag, X.; Münstedt, H. Thermorheological Behavior of Various Short-and Long-Chain Branched Polyethylenes

- and Their Correlations with the Molecular Structure. *Macromolecules* **2010**, *43* (17), 7341–7350.
- (13) Galland, G. B.; De Souza, R. F.; Mauler, R. S.; Nunes, F. F. ¹³C NMR Determination of the Composition of Linear Low-Density Polyethylene Obtained with [H₃-Methallyl-Nickel-Diimine]PF₆ Complex. *Macromolecules* **1999**, *32* (5), 1620–1625.
- (14) Dealy, J. M.; Larson, R. G.; Dealy, J. M.; Larson, R. G. *Structure and Rheology of Molten Polymers*; 2006.
- (15) Bourg, V.; Valette, R.; Moigne, N. Le; Ienny, P.; Guillard, V.; Bergeret, A. Shear and Extensional Rheology of Linear and Branched Polybutylene Succinate Blends. *Polymers* **2021**, *13* (4), 1–19.
- (16) Liang, X.; Luo, Z.; Yang, L.; Wei, J.; Yuan, X.; Zheng, Q. Rheological Properties and Crystallization Behaviors of Long Chain Branched Polyethylene Prepared by Melt Branching Reaction. **2017**.
- (17) Münstedt, H.; Kurzbeck, S.; Egersdörfer, L. Influence of Molecular Structure on Rheological Properties of Polyethylenes. *Rheologica Acta* **1998**, *29*, 21–29.
- (18) Zhou, Z.; Pesek, S.; Klosin, J.; Rosen, M. S.; Mukhopadhyay, S.; Cong, R.; Baugh, D.; Winniford, B.; Brown, H.; Xu, K. Long Chain Branching Detection and Quantification in LDPE with Special Solvents, Polarization Transfer Techniques, and Inverse Gated ¹³C NMR Spectroscopy. *Macromolecules* **2018**, *51* (21), 8443–8454.
- (19) Yu, Y.; Deslauriers, P. J.; Rohlfing, D. C. SEC-MALS Method for the Determination of Long-Chain Branching and Long-Chain Branching Distribution in Polyethylene. *Polymer* **2005**, *46* (14), 5165–5182.
- (20) Langsten, J. A.; Colby, R. H.; Chung, T. C. M.; Shimizu, F.; Suzuki, T.; Aoki, M. Synthesis and Characterization of Long Chain Branched Isotactic Polypropylene via Metallocene Catalyst and T-Reagent. *Macromolecules* **2007**, *40* (8), 2712–2720.
- (21) Gell, C. B.; Graessley, W. W.; Efstratiadis, V.; Pitsikalis, M.; Hadjichristidis, N. Viscoelasticity and Self-Diffusion in Melts of Entangled. *J Polym Sci Pol Phys* **1997**, *35*, 1943–1954.
- (22) Gabriel, C.; Lilge, D. Comparison of Different Methods for the Investigation of the Short-Chain Branching Distribution of LLDPE. *Polymer* **2001**, *42* (1), 297–303.
- (23) Zhou, Z.; Anklin, C.; Cong, R.; Qiu, X.; Kuemmerle, R. Long-Chain Branch Detection and Quantification in Ethylene–Hexene LLDPE with ¹³C NMR. *Macromolecules* **2021**, *54* (2), 757–762.
- (24) Dordinejad, A. K.; Jafari, S. H. A Qualitative Assessment of Long Chain Branching Content in LLDPE, LDPE and Their Blends via Thermorheological Analysis. *Journal of Applied Polymer Science* **2013**, *130* (5), 3240–3250.
- (25) Usanase, G.; Fraisse, F.; Taam, M.; Boyron, O. Determination of Short Chain Branching in LLDPE by Rheology. *Macromolecular Chemistry and Physics* **2022**, *223* (20), 2200150.

- (26) Touil, I. Multi-Micro/Nanolayers of Highly Mismatched Viscoelastic Polymers Based on Polyethylene with Varying Macromolecular Architectures: Multiscale Investigations towards Better Control of Their Structuration and Recycling by Coextrusion, 2021.
- (27) Lu, B. Rheology and Dynamics at the Interface of Multi Micro-/Nanolayered Polymers, 2017.
- (28) Lindeman, L. P.; Adams, J. Q. Carbon-13 Nuclear Magnetic Resonance Spectrometry: Chemical Shifts for the Paraffins through C9. *Analytical Chemistry* **1971**, *43* (10), 1245–1252.
- (29) Monrabal, B.; Sancho-Tello, J.; Mayo, N.; Romero, L. Crystallization Elution Fractionation. A New Separation Process for Polyolefin Resins. *Macromolecular Symposia* **2007**, *257*, 71–79.
- (30) Small, C. M.; McNally, G. M.; Murphy, W. R.; Marks, A. The Manufacture and Performance of Polyethylene-Polyisobutylene Films for Cling Applications. *Developments in Chemical Engineering and Mineral Processing* **2003**, *11* (1–2), 169–184.
- (31) Delgadillo-Velázquez, O.; Hatzikiriakos, S. G.; Sentmanat, M. Thermorheological Properties of LLDPE/LDPE Blends. *Rheologica Acta* **2008**, *47* (1), 19–31.
- (32) Liu, C.; He, J.; Ruymbeke, E. van; Keunings, R.; Bailly, C. Evaluation of Different Methods for the Determination of the Plateau Modulus and the Entanglement Molecular Weight. *Polymer* **2006**, *47* (13), 4461–4479.
- (33) Small, C. M.; McNally, G. M.; Murphy, W. R.; Marks, A. The Manufacture and Performance of Polyethylene-Polyisobutylene Films for Cling Applications. *Developments in Chemical Engineering and Mineral Processing* **2003**, *11* (1–2), 169–184.
- (34) Mohammadi, M.; Yousefi, A. A.; Ehsani, M. Thermorheological Analysis of Blend of High-and Low-Density Polyethylenes. *Journal of Polymer Research* **2012**, *19* (2), 24–29.
- (35) Micic, P.; Bhattacharya, S. N. Rheology of LLDPE, LDPE and LLDPE/LDPE Blends and Its Relevance to the Film Blowing Process. *Polymer International* **2000**, *49* (12), 1580–1589.
- (36) Delgadillo-Velázquez, O.; Hatzikiriakos, S. G.; Sentmanat, M. Thermorheological Properties of LLDPE/LDPE Blends. *Rheologica Acta* **2008**, *47* (1), 19–31.
- (37) Liu, C.; He, J.; Ruymbeke, E. van; Keunings, R.; Bailly, C. Evaluation of Different Methods for the Determination of the Plateau Modulus and the Entanglement Molecular Weight. *Polymer* **2006**, *47* (13), 4461–4479.
- (38) Wagner, M. H.; Laun, H. M. Nonlinear Shear Creep and Constrained Elastic Recovery of a LDPE Melt. *Rheologica Acta*. 1978, pp 138–148.
- (39) Malmberg, A.; Kokko, E.; Lehmus, P.; Löfgren, B.; Seppälä, J. V. Long-Chain Branched Polyethene Polymerized by Metallocene Catalysts Et[Ind]2ZrCl2/MAO and Et[IndH4]2ZrCl2/MAO. *Macromolecules* **1998**, *31* (24), 8448–8454.

- (40) Wingstrand, S. L.; Van Drongelen, M.; Mortensen, K.; Graham, R. S.; Huang, Q.; Hassager, O. Influence of Extensional Stress Overshoot on Crystallization of LDPE. *Macromolecules* **2017**, *50* (3), 1134–1140.
- (41) Wagner, M. H.; Kheirandish, S.; Yamaguchi, M. Quantitative Analysis of Melt Elongational Behavior of LLDPE/LDPE Blends. *Rheologica Acta* **2004**, *44* (2), 198–218.
- (42) Giunanca, R. The Effects of Long Chain Branching on the Rheological Properties of Polymers. **2002**, No. June, 82.

Supplementary Information for **Structure-rheology Properties of Polyethylenes with Varying Macromolecular Architectures**

Jixiang Li^a, Ibtissam Touil^a, Carlos Fernández de Alba^a, Fernande Boisson^a, Olivier Boyron^b, Esmail Narimissa^c, Bo Lu^d, Huagui Zhang^e, Abderrahim Maazouz^{a,f}, Khalid Lamnawar^{a,*}

^a *Université de Lyon, CNRS, UMR 5223, Ingénierie des Matériaux Polymères, INSA Lyon, F-69621, Villeurbanne, France*

^b *Université de Lyon, CNRS, UMR 5223, Ingénierie des Matériaux Polymères, UCBL, F-69621, Villeurbanne, France*

^c *Dept. of Chemical Engineering, Guangdong Technion–Israel Institute of Technology (GTIIT), Shantou 515063, China*

^d *Key Laboratory of Materials Processing and Mold (Ministry of Education), National Engineering Research Center for Advanced Polymer Processing Technology, Zhengzhou University, Zhengzhou 450002, China*

^e *College of Chemistry and Materials Science, Fujian Key Laboratory of Polymer Materials, Fujian Provincial Key Laboratory of Advanced Materials Oriented Chemical Engineering, Fujian Normal University, Fuzhou 350007, China*

^f *Hassan II Academy of Science and Technology, 10100 Rabat, Morocco*

** Corresponding author. E-mail address: khalid.lamnawar@insa-lyon.fr (K. Lamnawar).*

1. Supplementary Note 1 Extensional rheology

Extensional rheology was performed to probe the effect of long-chain branching (LCB) and short-chain branching (SCB) of the selected PEs and to understand the effect of molecular structures on their rheological properties. More recently, it has been proved that the elongational experiments are more sensitive to the long-chain branching than the classical characterization methods (SEC-malls...)[1].

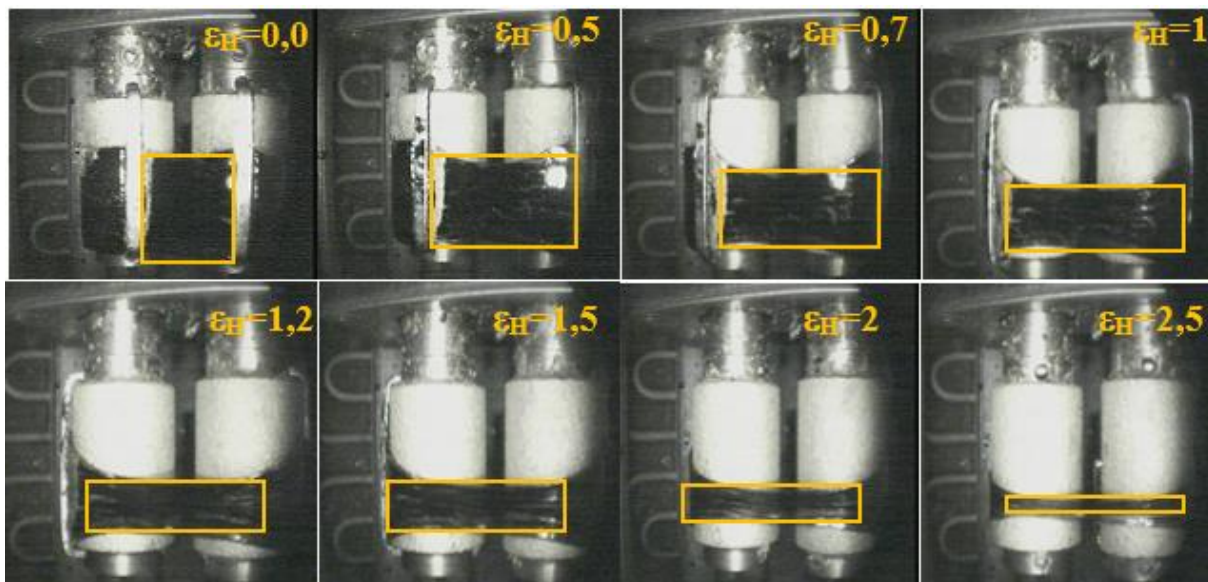


Figure S1 Sequential images recorded by the built-in camera to show the evolution of actual width dimension of neat polymer LL2 undergoing stretching at a constant Hencky strain rate of 0,1 s⁻¹

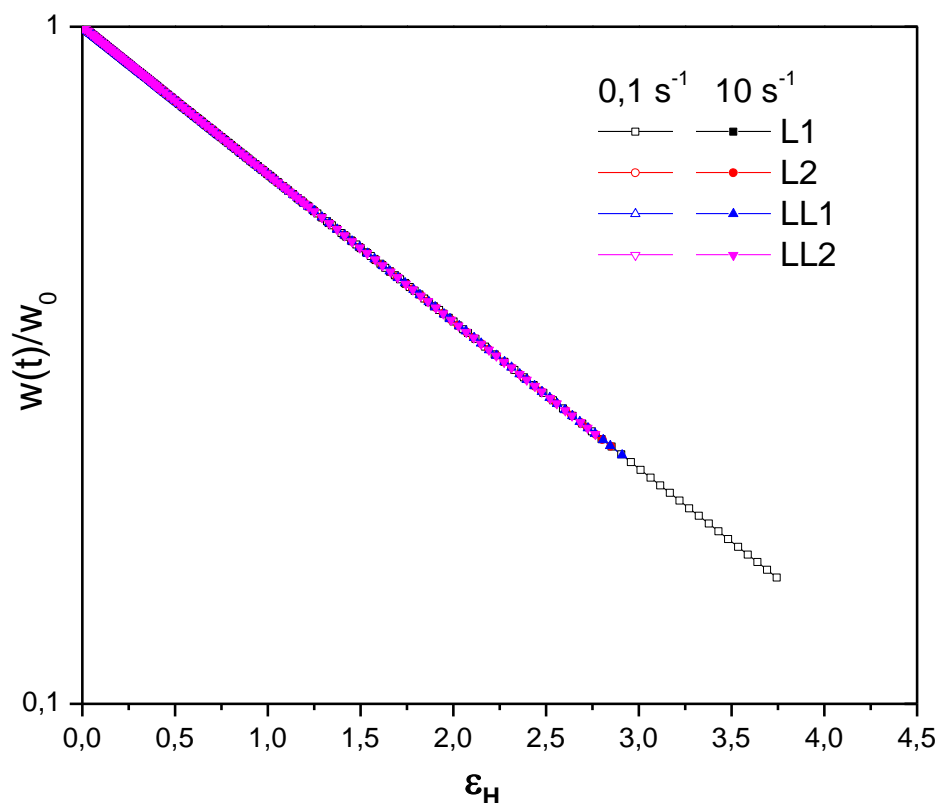


Figure S2 Width ratio for all PEs against the Hencky strain for two applied strain rates $0,1 \text{ s}^{-1}$ and 10 s^{-1}

2. Supplementary Note 2 SEC-LALS

The separation principle of SEC-Malls is described in Figure . The stationary phase is a porous gel in which small molecules will remain within the pores and flow more slowly, whereas large dissolved molecules will stay in the mobile phase and flow faster because they are too large to penetrate the pores, thus efficiently sorting the molecules by size. Then, each small fraction of polymer eluted out of the SEC column is analyzed instantly by the low-angle laser scattering LALS. The LALS term refers to the amount of scattered light by the samples at low angle detection and used to study the long-chain branching of PEs. This method is more sensitive to the presence of long-chain branching in high molecular weight polymers than the lower ones [2].

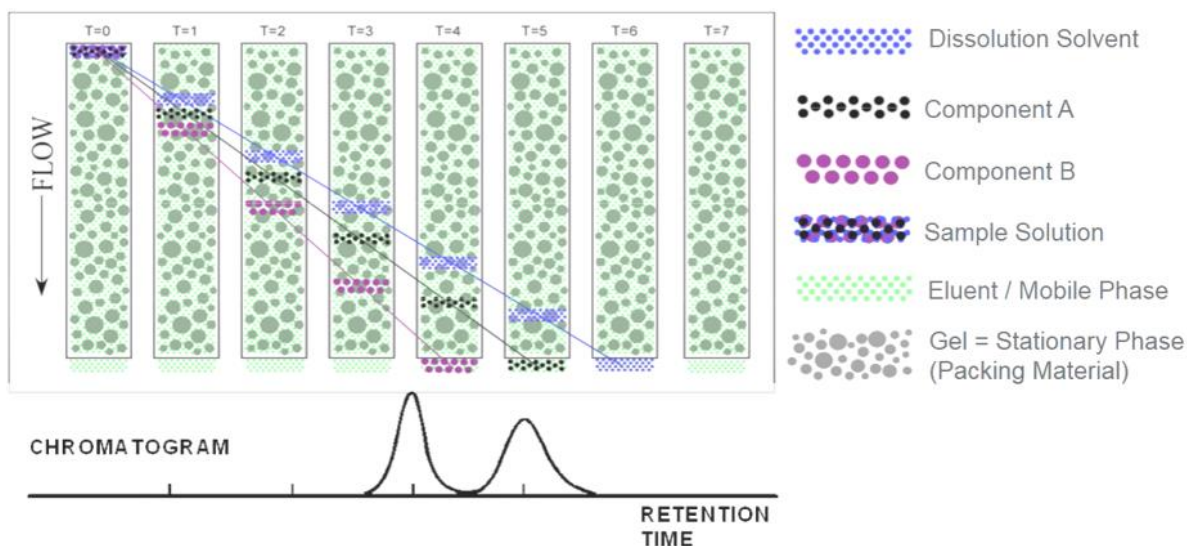


Figure S3 The separation principle of SEC

The absolute molecular weight and radius of gyration R_g of all PEs used in this study were measured directly by the SEC-LALS technique. Therefore, the long-chain branching distribution and content in the PEs were also determined by direct application of the Zimm–Stock approach [3].

3. Supplementary Note 3 Crystallization Elution Fractionation (CEF)

The advantage of CEF is to increase the physical separation obtained in the crystallization step and to reduce the fractionation time in the elution cycle, leading to a new extended separation as displayed in Figure . In CEF, the first step is the sample loading, followed by pumping a small flow of the solvent through the column over the cooling process[4]. The crystallization occurs at different places in the column and is maintained until the sample reaches its crystallization. Then, a new solvent flow F_e was inserted again as in TREF at an appropriate rate while the temperature is still increased. By raising the temperature of the column, the eluant dissolves the polymer components. A detailed description of this method is reported in the literature[5]. This method was used to support the information of the different PEs molecular architecture and branching structures determined by SEC and ^{13}C NMR.

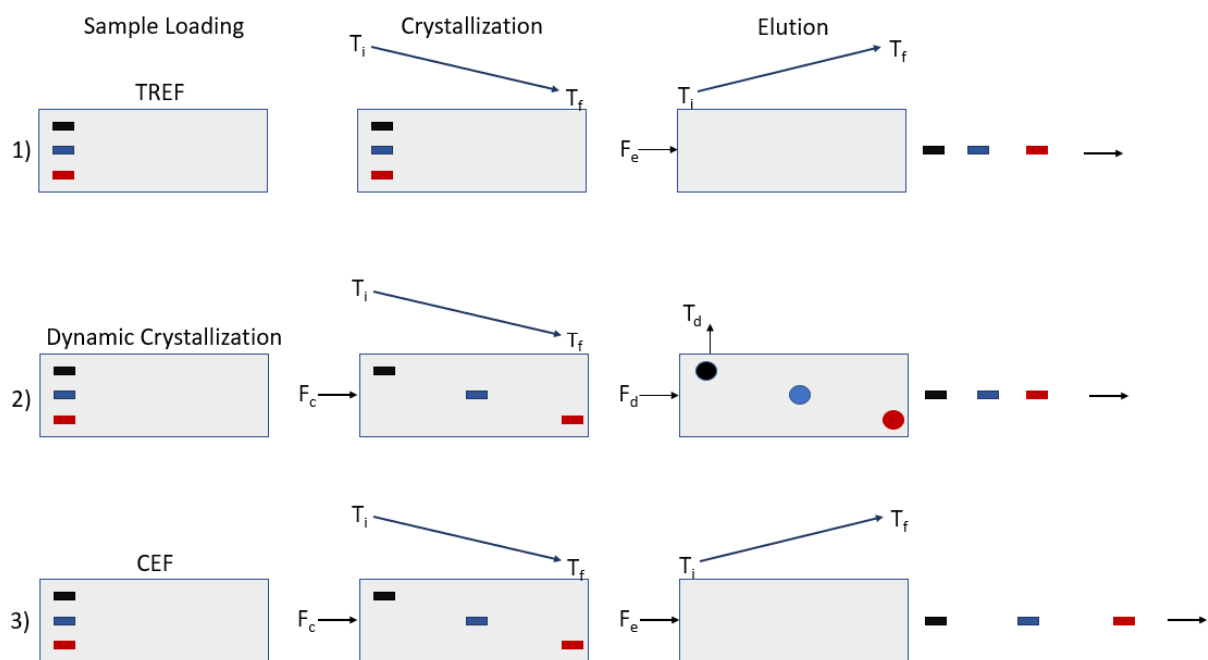


Figure S4 Scheme of the separations by crystallization_elution processes with T_i and T_f as the initial and final temperature of each step: 1) TREF separation process; 2) Dynamic crystallization process, 3) Crystallization Elution Fractionation process (B. Monrabal *et al.*, 2007).

4. Supplementary Note 4 ^{13}C -NMR and Randall model

According to the literature, the ethylene copolymerization with 1-hexene leads to establish butyl branches along the polyethylene backbone and has provided a useful NMR objective as a reference for characterizing the butyl branch being the most abundant branch seen in LDPE[6].

^{13}C -NMR chemical shifts assignments for all polyethylene used in this study were done according to Randall's previous work and were referenced here by setting the major methylene's backbone carbon resonances to 30.06 ppm[6]. The nomenclature used to identify the various backbone and branching carbons was shown in S5. It was based on Randall, Usami, and Takayama's previous work[7].

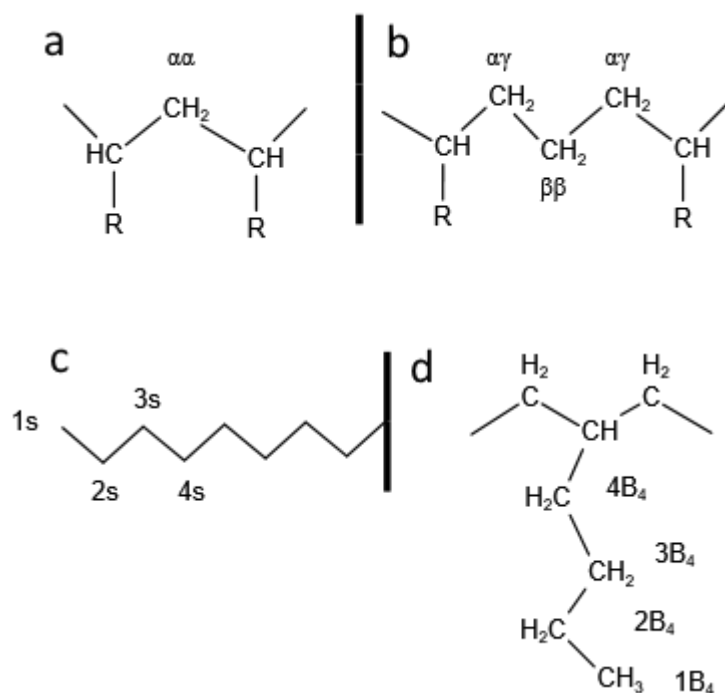


Figure S5 Nomenclature used for labelling the polymer backbone and side-chain carbons [10]

The backbone carbons are designated by a pair of Greek letters that indicate the position of the closest methylene carbons in each direction. The methine branch point is denoted by the carbon marked ‘br’ that can be easily isolated. The Greek symbol “α” denotes that methine carbon is bonded to a methylene carbon of concern. While two Greek symbols, “αα”, signify that the given methylene carbon is sandwiched between two methine carbons. Therefore, the “β” means that a methine carbon is two carbons removed from the carbon of concern, and so on with the Greek letters γ (3 carbons away) and δ. The linear alkyl end group is correspondingly labeled 1s, 2s, 3s, and 4s.

Additionally, the position of each carbon inside the different types of branches is identified by xB_n, where “n” denotes the branch's length and “x” designates the location of carbon inside the branch beginning with the methyl group as 1.

The presence of short-chain branching (SCB) can be identified from the “βδB_{1≤n≤4}” resonances located at 27.3 ppm and was observed for both LDPEs and LLDPEs. In the case of LLDPEs, the ββ_{HEH} carbons resonance identified at 24.1ppm was also to be taken into account for quantification. Even weaker resonances indicate the presence of a small amount of short-

chain branching. The equation below was thus used to measure the total number of short-chain branches " N_{SCB} " per 1000 carbons from signals integration of ^{13}C NMR spectra.

$$N_{SCB} = \frac{\left(\left(\frac{I_{\beta}}{2}\right) + I_{\beta\beta}\right)}{N_C} * 1000$$

, where " I_{β} " and " $I_{\beta\beta}$ " represent the integral value of each corresponding carbon signal, and " N_C " is the integral value of all the carbon signals of the spectra.

In addition, at the resonance at 32.2 ppm corresponding to " $3B_{n \geq 6}$ " carbons evidences long-chain branching. . Even weaker resonances indicate the presence of a small amount of long-chain branching. For both LDPEs and LLDPEs, the equation below was used to determine the total number of long-chain branches (N_{LCB}) per 1000C.

$$N_{LCB} = \frac{(I_{B_{n \geq 6}} * 1000)}{N_C}$$

where " $I_{B_{n \geq 6}}$ " denotes the measured integral value at 32.2 ppm and " N_C " corresponds to the integral value of all the carbon signals of the spectra.

Table S1 ^{13}C Chemical Shifts, peak assignments, and spectral integration for both LDPEs and LLDPEs

| Chemical Shift (ppm) | Assignment | Integral measurement | | | |
|----------------------|-------------------------------------|----------------------|------|-----------|-------|
| | | LDPE | | LLDPE | |
| | | L1 | L2 | LL1 | LL2 |
| 10.9 | 1B2 | 4.46 | 3.21 | - | 0.32 |
| 14 | 1S+1B4+1B6+1 B5 | 9.98 | 8.91 | 17.8 1 | 10.25 |
| 19.9 | 1B1 | 2.72 | 0.00 | | |
| 22.9 | 2S+2B5+2B ₆ ⁺ | 3.74 | 3.51 | 0.60 | 0.37 |

| | | | | | |
|-------|---|-------|------|------|--------|
| 23.4 | 2B4 | 8.69 | 7.96 | 21.2 | 11.50 |
| | | | | 6 | |
| 24.1 | $\beta\beta_{EHEHE}$ | 0 | 0 | 2.13 | 0.52 |
| 26.8 | 2B2+4B5 | 7.59 | 7.66 | 0.00 | 0.32 |
| 27.3 | $\beta\mathbf{B}_{n>4} + \beta\mathbf{B}_2$ | 27.86 | 22.7 | 40.1 | 27.36 |
| | | | 1 | 2 | |
| 27,48 | $\beta\mathbf{B}_1$ | 2 | 0 | 0 | 0 |
| 29.5 | 3B4 | | | | |
| 29.6 | 4S | | | | |
| 30 | [CH2]n | 1000 | 1000 | 100 | 1038.9 |
| | | | | 0 | 2 |
| 30 | $\gamma\mathbf{B}_{n>4} + \gamma\mathbf{B}_2$ | | | | |
| 31.1 | $\gamma\gamma_{HEEH}$ | | | | |
| 32.2 | 3S+3 \mathbf{B}_6^+ | 2.49 | 2.27 | 0.68 | 0.44 |
| 32.7 | 3B5 | 2.12 | 1.94 | 0.00 | 0.00 |
| 33.2 | CHB1 | 2.59 | 0.00 | 0.00 | 0.00 |
| 34 | 4B4+ $\alpha\mathbf{B}_2$ | | | | |
| 34.4 | $\alpha\mathbf{B}_{n>4}$ | 40.90 | 36.2 | 74.1 | 50.52 |
| | | | 8 | 9 | |
| 34.8 | 4HHH | | | | |
| 35.6 | brHHE | 1.81 | 0.98 | 2.64 | 0.00 |
| 37 | CH(1,3-)diB2 | 1.44 | 1.21 | 0.00 | |
| 37.5 | $\alpha\delta\mathbf{B}_1$ | 5.75 | 0.00 | | |
| 38 | CH \mathbf{B}^+4 | 11.61 | 9.58 | 22.0 | 15.90 |
| | | | | 7 | |
| 38.8 | $\alpha\alpha$ | | 1.04 | 1.03 | 0.37 |
| | | 2.08 | | | |
| 39.4 | xx | | 0.75 | 0.00 | 0.00 |

| | | | | |
|------------------------------|-------------|-------------|-------------|-------------|
| Total number of carbons (Nc) | 1137. 83 | 1108 .01 | 118 2.53 | 1156.7 9 |
|------------------------------|-------------|-------------|-------------|-------------|

4. Supplementary Note 5 ¹ Comparison between the predictions of the HMMSF model and Extensional rheology data

Modeling the shear and extensional rheological behaviors of polymers have been studied extensively to get detailed information on polymer molecular structure and processing behavior. On one hand, the KBKZ integral constitutive equation [8], one of the older models, has shown promising results in predicting polymer system shear and extensional rheological behaviors [9]. Samurkas *et al.* [10], on the other hand, demonstrated that the KBKZ model seems to be unable of simultaneously predicting the strain softening in shear and strain hardening in planar flows. Another research [11] used the Doi-Edwards theory [12] as well as the molecular stress function model [13] [14] to predict the extensional rheological behavior of linear and LCB polyethylene melts.

In a recent research, Wagner *et al.* [15–17] used the MSF model with two nonlinear material parameters to simulate the extensional viscosity growths. Masubuchi *et al.* [18] studied the molecular mobility in elongational flow by simulating primitive chain networks. They found good agreement between models and experimental data of monodisperse linear and pom-pom branched polystyrene. Narimissa *et al.* [19–21] developed a hierarchical multimode stress function (HMMSF) model to predict the rheological behaviors of linear and LCB polymers for different types of flow including uniaxial extensional, multiaxial extensional, and shear deformations. This HMMSF model is based on hierarchical relaxation, dynamic dilution, interchain tube pressure, and convective constraint release [22]. The model's findings match well with those obtained from elongational viscosity data for a variety of LCB polymer melts and present an opportunity for estimating the morphology as well as the crystallization rate of HDPE [23].

The aim of this part is to compare the HMMSF model to the obtained extensional rheological data of both sets of LDPEs and LLDPEs. So far, we've only worked with two types of LDPE at 150°C, and therefore the remainder LLDPEs will be modeled soon. More details

about the HMMSF modelling approach can be found in the [22]. Figure 20 compares the measured extensional viscosity of LDPE-L1 and LDPE-L2 at 150°C to the HMMSF model's predictions. As we can observe the HMMSF model and the extensional viscosity data of both LDPEs show good agreement. The slight deviation observed for LDPE-L2 for 0,005 s⁻¹ is possibly attributed to a measurement error.

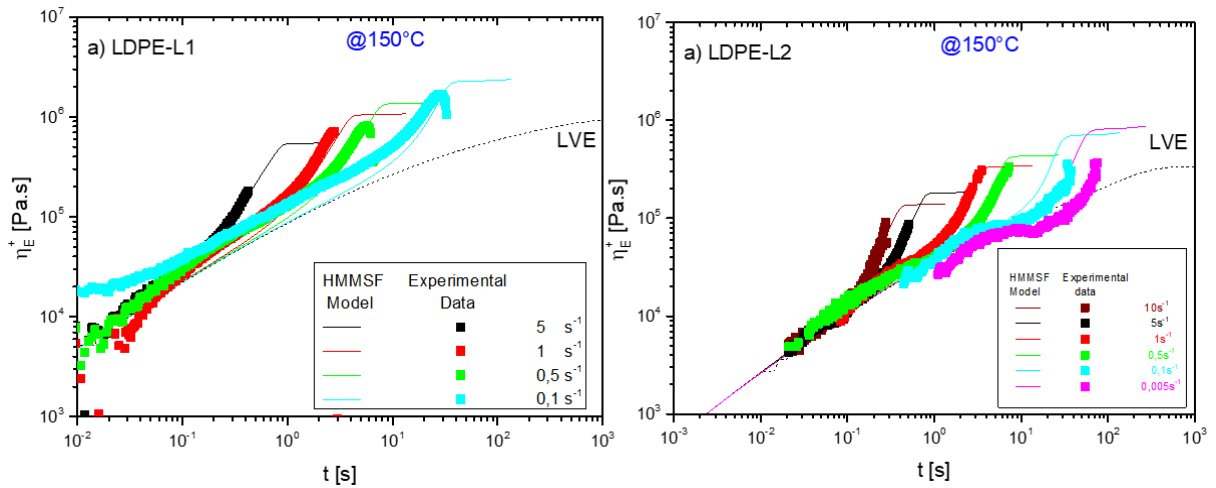


Figure S6 Comparison between the predictions of the HMMSF model (continuous lines) and measurements of Extensional rheology (symbols) at 150°C.

Reference

1. Narimissa, E.; Wagner, M.H. From Linear Viscoelasticity to Elongational Flow of Polydisperse Linear and Branched Polymer Melts: The Hierarchical Multi-Mode Molecular Stress Function Model. *Polymer* **2016**, *104*, 204–214, doi:10.1016/j.polymer.2016.06.005.
2. Yu, Y.; Deslauriers, P.J.; Rohlfiing, D.C. SEC-MALS Method for the Determination of Long-Chain Branching and Long-Chain Branching Distribution in Polyethylene. *Polymer* **2005**, *46*, 5165–5182, doi:10.1016/j.polymer.2005.04.036.
3. Zimm, B.H.; Stockmayer, W.H. The Dimensions of Chain Molecules Containing Branches and Rings. *The Journal of Chemical Physics* **1949**, *17*, 1301–1314, doi:10.1063/1.1747157.
4. Pasch, H.; Malik, M.I. Crystallization-Based Fractionation Techniques. In *Advanced Separation Techniques for Polyolefins*; Pasch, H., Malik, M.I., Eds.; Springer International Publishing: Cham, 2014; pp. 11–73 ISBN 978-3-319-08632-3.
5. Monrabal, B.; Sancho-Tello, J.; Mayo, N.; Romero, L. Crystallization Elution Fractionation. A New Separation Process for Polyolefin Resins. *Macromolecular Symposia* **2007**, *257*, 71–79, doi:10.1002/masy.200751106.
6. Randall, J.C. A REVIEW OF HIGH RESOLUTION LIQUID ¹³C NUCLEAR MAGNETIC RESONANCE CHARACTERIZATIONS OF ETHYLENE-BASED POLYMERS. *Journal of Macromolecular science, Part C: Polymer Reviews* **1989**, *29*, 201–317, doi:http://dx.doi.org/10.1080/07366578908055172.
7. Usami, T.; Takayama, S. Fine-Branching Structure in High-Pressure, Low-Density Polyethylenes by 50.10-MHz ¹³C NMR Analysis. *Macromolecules* **1984**, *17*, 1756–1761, doi:10.1021/ma00139a022.
8. Kaye, A. NON-NEWTONIAN FLOW IN INCOMPRESSIBLE FLUIDS Part I A General Rheological Equation of State Part II Some Problems in Steady Flow By. *Aerospace Engineering reports, Technical University of Delft* **1962**, 1–20.
9. Tanner, R.I. From A to (BK)Z in Constitutive Relations. *Journal of Rheology* **1988**, *32*, 673–702, doi:10.1122/1.549986.

10. Samurkas, T.; Dealy, J.M.; Larson, R.G. Strong Extensional and Shearing Flows of a Branched Polyethylene. *Journal of Rheology* **1989**, *33*, 559–578, doi:10.1122/1.550028.
11. Wagner, M.H.; Bastian, H.; Ehrecke, P.; Hachmann, P.; Meissner, J. A Constitutive Analysis of Uniaxial, Equibiaxial and Planar Extension of Linear and Branched Polyethylene Melts. *Progress and Trends in Rheology V* **1998**, 4–7, doi:10.1007/978-3-642-51062-5_2.
12. Doi M, E.S. The Theory of Polymer Dynamics. *Oxford University Press, Oxford* **1986**.
13. Wagner, M.H.; Schaeffer, J. Nonlinear Strain Measures for General Biaxial Extension of Polymer Melts. *Journal of Rheology* **1992**, *36*, 1–26, doi:10.1122/1.550338.
14. Wagner, M.H.; Schaeffer, J. Rubbers and Polymer Melts: Universal Aspects of Nonlinear Stress–Strain Relations. *Journal of Rheology* **1993**, *37*, 643–661, doi:10.1122/1.550388.
15. Wagner, M.H.; Rubio, P.; Bastian, H. The Molecular Stress Function Model for Polydisperse Polymer Melts with Dissipative Convective Constraint Release. *Journal of Rheology* **2001**, *45*, 1387–1412, doi:10.1122/1.1413503.
16. Wagner, M.H.; Yamaguchi, M.; Takahashi, M. Quantitative Assessment of Strain Hardening of Low-Density Polyethylene Melts by the Molecular Stress Function Model. *Journal of Rheology* **2003**, *47*, 779–793, doi:10.1122/1.1562155.
17. Wagner, M.H.; Hepperle, J.; Münstedt, H. Relating Rheology and Molecular Structure of Model Branched Polystyrene Melts by Molecular Stress Function Theory. *Journal of Rheology* **2004**, *48*, 489–503, doi:10.1122/1.1687786.
18. Masubuchi, Y.; Matsumiya, Y.; Watanabe, H.; Marrucci, G.; Ianniruberto, G. Primitive Chain Network Simulations for Pom-Pom Polymers in Uniaxial Elongational Flows. *Macromolecules* **2014**, *47*, 3511–3519, doi:10.1021/ma500357g.
19. Narimissa, E.; Rolón-Garrido, V.H.; Wagner, M.H. A Hierarchical Multi-Mode MSF Model for Long-Chain Branched Polymer Melts Part I: Elongational Flow. *Rheologica Acta* **2015**, *54*, 779–791, doi:10.1007/s00397-015-0879-2.

20. Narimissa, E.; Wagner, M.H. From Linear Viscoelasticity to Elongational Flow of Polydisperse Linear and Branched Polymer Melts: The Hierarchical Multi-Mode Molecular Stress Function Model. *Polymer* **2016**, *104*, 204–214, doi:10.1016/j.polymer.2016.06.005.
21. Narimissa, E.; Wagner, M.H. A Hierarchical Multimode Molecular Stress Function Model for Linear Polymer Melts in Extensional Flows. *Journal of Rheology* **2016**, *60*, 625–636, doi:10.1122/1.4953442.
22. Narimissa, E.; Wagner, M.H. Review of the Hierarchical Multi-Mode Molecular Stress Function Model for Broadly Distributed Linear and LCB Polymer Melts. *Polymer Engineering and Science* **2019**, *59*, 573–583, doi:10.1002/pen.24972.
23. Poh, L.; Narimissa, E.; Wagner, M.H. Modelling of Elongational Flow of Hdpe Melts by Hierarchical Multi-Mode Molecular Stress Function Model. *Polymers* **2021**, *13*.